Single-molecule fluorescence spectroscopy of protein folding

Benjamin Schuler and Daniel Nettels, Biochemisches Institut, Universität Zürich, Zürich, Switzerland

This is an update of B. Schuler, D. Nettels, 3.6 Single-Molecule Spectroscopy of Protein Folding, Editor(s): Edward H. Egelman, Comprehensive Biophysics, Elsevier, 2012, Pages 115–137, ISBN 9780080957180, https://doi.org/10.1016/B978-0-12-374920-8.00306-4.

Key points

- Single-molecule spectroscopy, especially in combination with Förster resonance energy transfer (FRET) has become an important method for investigating protein folding.
- Particular strengths of the technique are that it avoids ensemble averaging, enables the separation of subpopulations even in heterogeneous systems and complex environments, and provides access to dynamics across a wide range of timescales.
- Areas in protein folding where single-molecule spectroscopy has turned out to be particularly powerful are unfolded state structure and dynamics, measurements of transition paths, the observation of rare events, the mechanisms of complex folding reactions, and the role of the cellular protein folding machinery.
- The field of single-molecule spectroscopy keeps advancing rapidly, for instance by integrating experimental and computational techniques.

Glossary

Single-molecule spectroscopy Optical detection of individual molecules, most commonly using fluorescence.

Förster resonance energy transfer (FRET) Non-radiative transfer of excitation energy between two molecular entities ("donor" and "acceptor") separated by distances considerably exceeding the sum of their van der Waals radii in the very weak dipole–dipole coupling limit. In most biophysical applications, both donor and acceptor are fluorescent.

Energy transfer efficiency (E) Probability of FRET from the donor to the acceptor chromophore. In single-molecule experiments, E is usually determined either from the fraction of emitted acceptor photons over the total number of photons, or from fluorescence lifetimes.

Fluorescence correlation spectroscopy (FCS) Statistical analysis of fluctuations in fluorescence intensity or count rates via time correlation. FCS is a broadly applicable way of assessing biomolecular dynamics over a broad range of timescales.

Markov process A random process whose future state probabilities are determined by its most recent state only (a "memoryless" process).

Confocal fluorescence detection An optical configuration common in single-molecule detection and FCS, which uses point illumination by the focal volume of the exciting laser beam in combination with a pinhole in the optically conjugate plane in front of the detector to eliminate out-of-focus fluorescence.

Total internal reflection fluorescence (TIRF) An optical configuration common in single-molecule detection, where the evanescent field formed by a totally internally reflected laser beam is used to excite molecules close to an interface, which can then be imaged onto a detector, usually a highly sensitive camera.
Transition paths The successful reactant-to-product crossing of the free-energy barrier separating two free-energy minima, such as the folded and unfolded states in protein folding. Transition paths are rare events with very short duration and thus challenging to resolve experimentally.

Abstract

Single-molecule fluorescence spectroscopy has developed into a versatile method for probing distances, distance distributions, and dynamics in proteins, especially in combination with Förster resonance energy transfer (FRET). These studies have produced novel and important information on questions in protein folding that have been impossible or difficult to address with ensemble measurements. Here, we present some basic concepts of single-molecule spectroscopy and summarize advances it has enabled in the field of protein folding.

Introduction

We are used to depicting chemical reactions and biochemical processes in terms of individual molecules. We do so at various levels of complexity, ranging from simple textbook cartoons to the atomic detail of molecular dynamics simulations. But until recently, the vast majority of our knowledge about these systems had been derived from experiments on large ensembles of molecules, which yield only average values of observable properties. The sequence of molecular events describing the underlying reactions is typically inferred from testing a model by systematic variation of parameters. For kinetic ensemble studies, the reactions need to be synchronized, which is often difficult. The concept of observing single molecules is particularly appealing for processes with a large degree of conformational and dynamic heterogeneity, protein folding being a case in point.

Only since the turn of the millennium has it become feasible to investigate the folding of single protein molecules. These techniques offer a fundamental advantage beyond our mere fascination for the direct observation of molecular processes: they can resolve and quantify the properties of individual molecules or subpopulations inaccessible in ensemble experiments. Fluorescence spectroscopy is a particularly appealing technique, owing to its extreme sensitivity and versatility. With Förster resonance energy transfer (FRET), we can investigate intramolecular distance distributions and conformational dynamics of single protein molecules. In combination with fluctuation methods such as fluorescence correlation spectroscopy (FCS), it is possible to obtain detailed insights into the dynamic processes of protein folding down to the timescales of fluorescence photophysics in the nanosecond range. In the following overview, we will first present some of the history and the basic concepts underlying single-molecule experiments, then we will illustrate the type of results obtained from optical single-molecule experiments to date, and finally we will provide a perspective on current developments and future directions in the field.

History and principles of single-molecule detection

Remarkably, the very first single molecules that were detected appear to have been proteins. In 1970, step-like changes in ion conductance were observed for artificial lipid films containing small numbers of gramicidin A molecules (Hladky and Haydon, 1970). Since then, the recording of such signals from single channels has matured to a method that now dominates the investigation of ion channels (Sakmann and Neher, 1995). Owing to this long tradition, the single-channel field provides a wealth of examples and analysis methods for the stochastic chemical kinetics observed in single molecules.

A very different type of methods enabled the first observation of single atoms and molecules on surfaces in the early 1980s: scanning tunneling microscopy and atomic force microscopy (AFM) (Binnig et al., 1986), where a sharp tip is used to probe the surface of a sample with atomic resolution. The simplicity of the instrumentation quickly made AFM a standard method, and soon it allowed the imaging of samples in solution (Drake et al., 1989), including proteins. In 1997, the mechanical unfolding of individual domains of titin molecules was reported, both with AFM (Rief et al., 1997) and laser tweezers (Kellermayer et al., 1997; Tskhovrebova et al., 1997). The investigation of proteins under mechanical force has made completely new aspects of protein folding and stability accessible that cannot be studied in ensemble experiments and has reached remarkable resolution of detail and time resolution (Petrosyan et al., 2021; Zoldak and Rief, 2013).

The optical detection of single molecules dates back to the 1970s, when it became possible to measure fluorescence from single atoms in dilute atomic beams in the gas phase, where the background problem is minimal. Observing single molecules in the condensed phase is much more difficult, because Rayleigh and Raman scattering produce a large background. An additional source of unwanted signal are contaminants, which make great demands on the purity of the matrix. Moreover, an atom in vacuum is

a chemically very stable system, even in its excited state, whereas fluorescent molecules in the condensed phase survive only a limited number of excitation-emission cycles before they are irreversibly destroyed—a process termed photobleaching. Single-molecule detection in a solid or liquid matrix therefore requires additional measures. First of all, an optical method must be used that provides as strong a signal from an individual molecule as possible relative to background from the large number of matrix molecules. The most popular option is fluorescence, where a dye molecule resonantly interacts with the excitation light. Due to the Stokes shift, the emitted light can be selected spectrally, typically with interference filters. To aid the signal from an individual molecule to be observed against the background signal from matrix molecules, it is helpful to reduce the size of the detection volume as much as possible, because the background level is proportional to the number of matrix molecules in the observed volume. Such spatial selection can be achieved, for instance, by very tightly focusing a laser beam into the sample, combined with confocal detection, or by total internal reflection fluorescence (TIRF) microscopy (cf. Section **Kinetics: From Ensembles to Single Molecules**).

The first detection of individual chromophores in solid matrices was achieved at liquid helium temperature with modulated absorption spectroscopy in 1989 (Moerner and Kador, 1989). Soon after, fluorescence spectroscopy was shown to yield superior signal-to-noise (Orrit and Bernard, 1990). Within a few years, successful fluorescence experiments at room temperature followed (Ambrose et al., 1994; Betzig and Chichester, 1993; Macklin et al., 1996; Nie et al., 1994; Xie and Dunn, 1994), leading to an explosion of the field, and opening the way for single-molecule detection of suitably labeled biomolecules. The introduction of FCS with a confocal detection scheme (Rigler et al., 1993) and single-molecule sensitivity was another important step for single-molecule studies in solution. The demonstration of FRET in individual, labeled DNA molecules (Ha et al., 1996) triggered a revival of this "spectroscopic ruler" (Stryer, 1978; Stryer and Haugland, 1967), enabling distance measurements in single biomolecules. The strongly distance-dependent nonradiative energy transfer between an acceptor and a donor chromophore (Förster, 1948) had been used to study protein folding and dynamics for decades (Haas, 2005), and indeed, the first experiments applying single-molecule FRET to protein folding followed soon (Deniz et al., 2000; Jia et al., 1999; Schuler et al., 2002; Talaga et al., 2000). Especially the ability of the method to separate subpopulations, e.g., folded and unfolded protein molecules, and its potential to investigate intramolecular dynamics and rare events has made it into an important method in the field of single-molecule protein folding (Banerjee and Deniz, 2014; Nettels et al., 2024; Schuler and Eaton, 2008).

Kinetics: from ensembles to single molecules

Assuming an infinitely large homogeneous[1] system (a good approximation for a standard protein folding experiment in a test tube[2]) consisting of a set of n subpopulations (thermodynamic states) separated by sufficiently large free-energy barriers, the concentrations of molecules assigned to these states will evolve in time according to a set of coupled, first order, ordinary differential equations: the reaction rate equations. The overall reaction is thus treated as a continuous process using deterministic mathematical concepts. The time course of the reaction will be described by a sum of n-1 exponential terms. Their individual time constants, however, will be complex algebraic expressions of all the rate constants in the mechanism and therefore have, in general, no simple physical significance.

But at the molecular level, the system is of course neither continuous nor deterministic. It is discrete, because molecules come in integer numbers, and molecular populations only change by integer amounts. Moreover, the system is stochastic, because the transitions of individual molecules from one state to another are ultimately initiated by thermal fluctuations and molecular collisions. If we observe the signal from a sufficiently small number of molecules, these fluctuations about the average behavior become large enough to be measured, and can be used to extract dynamic information about the system, an insight conceived in the context of light scattering experiments (Berne and Frisch, 1967; Blum and Salsburg, 1968; Magde et al., 1972; Yeh and Keeler, 1969) and membrane channel recordings (Katz and Miledi, 1970), and now used routinely, for instance in FCS (Magde et al., 1972; Rigler and Elson, 2001a; Rigler et al., 1993) (cf. Section **Correlation Analysis**). Suppose, for example, we observe $N = 1000$ protein molecules under conditions corresponding to the unfolding midpoint. The probability of an individual molecule being folded is $p = 0.5$, so the variation in the number of folded molecules is given by the standard deviation of the binomial distribution as $[N\ p\ (1\ -\ p)]^{1/2} \approx 16$. The number of protein molecules that are folded at equilibrium is therefore not constant, but is 500 ± 16, where the standard deviation reflects the random fluctuations in the number of folded molecules from instant to instant.

The smaller the number of molecules we observe, the larger the relative fluctuations of the signal will be. Ultimately, if only a single molecule is observed, we expect approximately step-like transitions between the states the molecule can populate. In the simplest example of a two-state folding reaction:

$$U \underset{k_u}{\overset{k_f}{\rightleftarrows}} F \tag{1}$$

If equilibration within each state is fast relative to the transition rates between the states, the molecule will reside in either the folded (F) or the unfolded state (U) for extended periods of time, with intermittent rapid jumps between them, the transition paths (see

[1] "Homogeneous" is used here in the chemical sense, denoting a well-mixed solution.
[2] 100 μL of a 1 μM sample still contain $6 \cdot 10^{13}$ molecules.

Section Protein Folding Trajectories, Kinetics, and Transition Paths). How can we extract kinetic information from such single-molecule trajectories (Fig. 1A,B)?

In classical chemical kinetics, the interconversion between states is described in terms of changes in concentrations or large numbers of molecules in the sample volume with respect to time. For the simple two-state reaction above (Eq. (1)), the kinetic mechanism is encoded in the reaction rate equations

$$\frac{dN_U(t)}{dt} = -k_f N_U(t) + k_u N_F(t) \quad \text{and} \quad \frac{dN_F(t)}{dt} = -k_u N_F(t) + k_f N_U(t), \tag{2}$$

with the number of molecules in the folded and unfolded state, N_F and N_U, respectively, and the folding and unfolding rate coefficients, k_f and k_u, respectively. This set of differential equations can be solved given suitable initial conditions. For instance, with $N_U(0) = N$ and $N_F(0) = 0$, we obtain

$$N_F(t) = N\frac{k_f}{k_f + k_u}\left(1 - e^{-(k_f+k_u)t}\right) \quad \text{and} \quad N_U(t) = N - N_F(t). \tag{3}$$

In ensemble protein folding kinetics, measurements typically involve perturbations, e.g., by rapid mixing or temperature jump. The chosen kinetic model can then be tested by using this solution of the reaction rate equations to describe the relaxation to equilibrium.

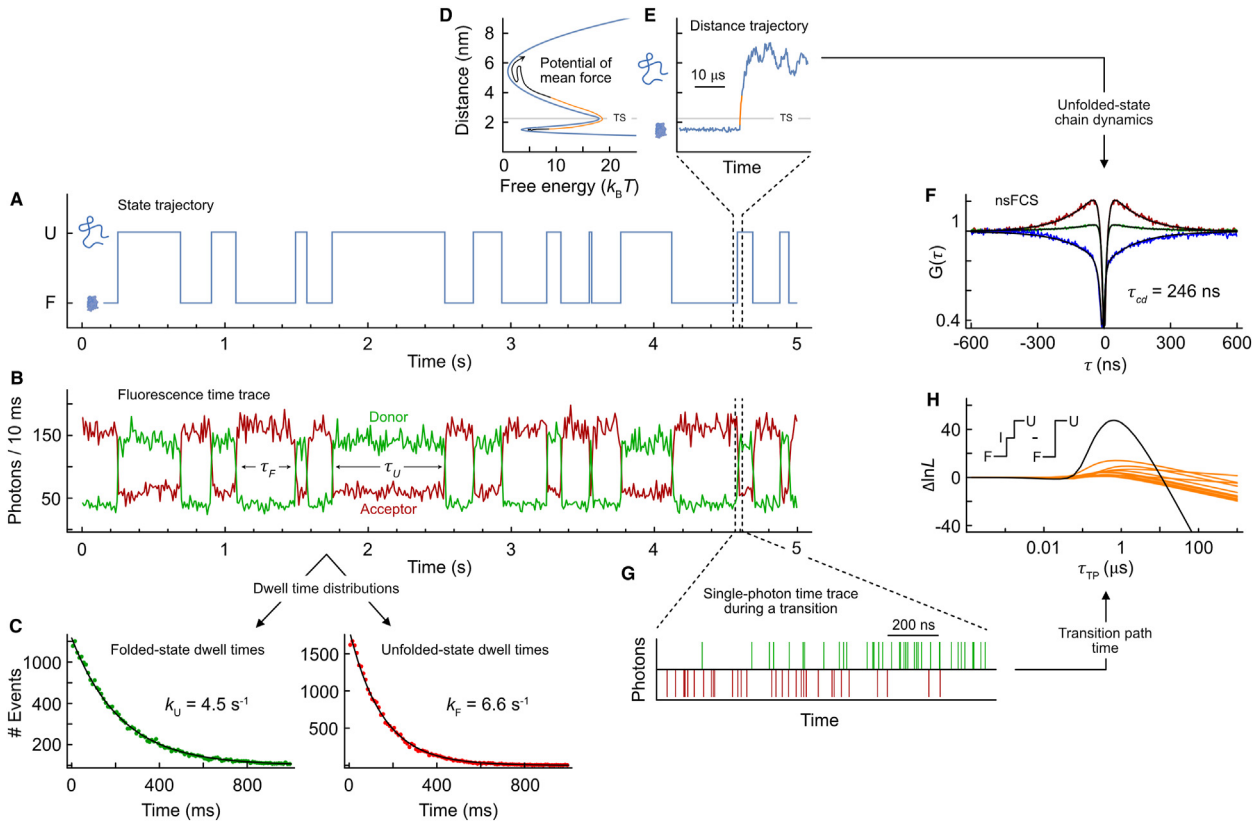

Fig. 1 Probing different aspects of protein folding dynamics with single-molecule FRET spectroscopy, illustrated for apparent two-state dynamics between folded (F) and unfolded state (U). (A) A two-state trajectory and (B) the corresponding photon emission from donor (green) and acceptor (red), with (C) the resulting exponential dwell time distributions identified with the Viterbi algorithm (Viterbi, 1967). (D) A 1D free-energy surface of the process (TS: transition state) with (E) the diffusive dynamics on this potential near a transition (orange segment: transition path). (F) Rapid distance dynamics in the unfolded state can be probed with nanosecond FCS (nsFCS; donor and acceptor autocorrelations: green and red, respectively; crosscorrelation: blue; fits: black lines). τ_{cd}, the mean correlation time of the chain dynamics, is obtained from fitting the curves. (G) Time-resolved recording of photon emission during a transition (example using 30 MHz average count rate, a regime that is starting to come into reach (Grabenhorst et al., 2024)) can be used for (H) a likelihood-based analysis of transition path times (Chung et al., 2012). $\Delta\ln L$ is the difference between the log-likelihoods for a model that assumes a virtual intermediate (I) mimicking a transition state of finite lifetime and for an instantaneous transition, yielding in this example a most likely transition path time, τ_{TP}, of ~1 µs (orange: results from ten individual photon time traces; black: sum). The data shown were simulated based on a two-state Markov model (A, B), or in terms of diffusion on a free-energy surface by discretizing the potential and using a discrete random walk with microscopic rate coefficients (E–G). Note that higher photon rates were used for simulating (G) than for (B).

If we want to describe the kinetics observed for a single molecule, it may at first not be obvious how the reaction rate equations and their solution could apply, since we do not have any changes in concentrations or numbers of molecules, and instead of a continuous, deterministic process, we are dealing with a discontinuous, stochastic process. However, we can save the day by writing **Eq. (2)** in terms of the probabilities $p_U = N_U/N$ and $p_F = N_F/N$ of being in the unfolded or folded state, respectively[3]:

$$\frac{dp_U(t)}{dt} = -k_f p_U(t) + k_u p_F(t) \quad \text{and} \quad \frac{dp_F(t)}{dt} = -k_u p_F(t) + k_f p_U(t), \tag{4}$$

with solutions analogous to **Eq. (3)**, i.e., $p_U(t) = N_U(t)/N$ and $p_F = N_F(t)/N$. Instead of describing changes in concentrations or numbers of molecules, we can thus use the same mathematical framework to describe changes in probabilities of being in the states involved. In the context of probabilistic reactions, **Eq. (4)** are referred to as the Master equations (Makarov, 2015).

As an example, let us assume we observe a molecule that is in the unfolded state at time $t = 0$, and we would like to know how long it will remain in the unfolded state until it jumps to the folded state, which we refer to as the dwell time or survival time in the unfolded state. If we ignore the possibility of the reaction back to the unfolded state, this is equivalent to the irreversible reaction U → N, in which case **Eq. (4)** simplifies to

$$\frac{dp_U(t)}{dt} = -k_f p_U(t). \tag{5}$$

with the initial condition $p_U(0) = 1$, we obtain the solution $p_U(t) = e^{-k_f t}$, which is referred to as the survival probability. The exponential distribution demonstrates that short dwell times are more likely than long dwell times, and that the probability of being in the unfolded state converges to zero for long times. The probability that the protein "survives" in the unfolded state up to time t and then folds in the next short time interval dt is given by $k_f p_U(t)dt$. Hence, we introduce the transition probability density

$$p_{U\to F}(t) = k_f e^{-k_f t}, \tag{6}$$

which is normalized so that its integral between 0 and infinity equals 1. The average dwell time in the unfolded state then results as

$$\langle t_U \rangle = \int_0^\infty t p_{U\to F}(t)dt = 1/k_f = \tau_U. \tag{7}$$

This relation between dwell times and rate coefficient illustrates the close link between the familiar concepts from ensemble kinetics and the behavior of individual molecules. The average dwell times in the folded and unfolded states are given by the inverse rate coefficients of unfolding, k_u, and folding, k_f, respectively (**Fig. 1**C). Such simple stochastic chemical kinetics are indeed observed for single immobilized protein molecules (Chung et al., 2009; Rhoades et al., 2004).

Finally, at equilibrium, we have $dp_U/dt = dp_F/dt = 0$, so we obtain from **Eq. (4)** the folding equilibrium constant

$$K = \frac{k_f}{k_u} = \frac{\tau_F}{\tau_U} = \frac{p_F^{eq}}{p_U^{eq}},$$

where p_F^{eq} and p_U^{eq} are the equilibrium probabilities of being in states F and U, respectively, which are proportional to the average dwell times in the two states and can thus be obtained directly from single-molecule trajectories. Long single-molecule recordings thus enable the analysis of the kinetic and thermodynamic properties of individual molecules without ensemble averaging and can reveal kinetic heterogeneity that would be difficult to detect otherwise, e.g., in multi-domain protein folding or in systems involving peptidyl-prolyl cis-trans isomerisation (Stigler et al., 2011; Zosel et al., 2018).

Correlation analysis

A powerful method to investigate dynamics and distance fluctuations across a broad range of timescales is fluorescence correlation spectroscopy (FCS) (Rigler and Elson, 2001b). According to the fluctuation-dissipation theorem (Callen and Welton, 1951), the rates of relaxation of a system to equilibrium after a small perturbation are described by the same rate coefficients as the time correlation of spontaneous fluctuations of the undisturbed system. Correlation spectroscopy can therefore provide information about the kinetics of reactions or molecular dynamics even at equilibrium.

The central quantity for analyzing such fluctuations and their loss of coherence are correlation functions (Berne and Pecora, 2000). The time correlation between two observables A and B is defined as[4]

[3]Here we implicitly assume that the system is ergodic, i.e., that the probabilities of being in state U and F are independent of whether we observe a single molecule for a long time or whether we observe a snapshot in time of a large ensemble of molecules. Ergodicity breaking can occur if there is static heterogeneity in an ensemble, i.e., if the interconversion between states is slower than the observation time of a single molecule (Hyeon et al., 2012).
[4]Here we again assume the system to be ergodic. Additionally, we assume that the system is at equilibrium, so that the averaging is independent of the starting time, $t = 0$.

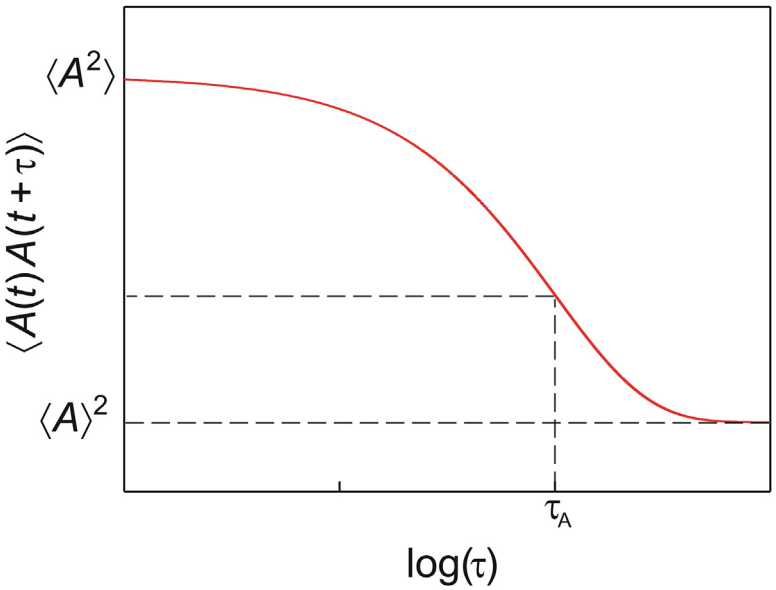

Fig. 2 A general, unnormalized autocorrelation function of signal *A* with correlation time τ_A (see text for details). From Fig. 7.3 in Schuler, B. From Protein Folding in Ensembles to Single Molecules, in: Protein folding, misfolding and aggregation: Classical themes and novel approaches; Muñoz, V. Ed.; RSC Publishing: Cambridge, 2008, pp. 139–156.

$$\langle A(t)B(t+\tau)\rangle = \lim_{T\to\infty}\frac{1}{T}\int_0^T A(t)B(t+\tau)dt. \tag{8}$$

(In any experimental measurement, the averaging is over a finite time, but the observation time T needs to be longer than the timescale of the process of interest.) If an observable is correlated with itself, i.e., if $A = B$, we have an autocorrelation, otherwise it is a cross-correlation between different properties or signals, e.g., fluorescence emission from a donor and an acceptor chromophore undergoing FRET. The autocorrelation function of a non-conserved, non-periodic property decays from its initial value $\langle A^2\rangle$ to the final value $\langle A\rangle^2$ with a time constant characteristic of the fluctuation of A, where the value at time t, $A(t)$, and the value at a later time $t+\tau$, $A(t+\tau)$, are expected to become uncorrelated at long lag times τ (**Fig. 2**). In some cases, the autocorrelation function decays exponentially, with a characteristic *relaxation time* or *correlation time*, but often it takes a more complex functional form. The most common example is an FCS experiment where fluorescently labeled molecules diffuse through a confocal volume approximated as a three-dimensional Gaussian shape.[5] The simplest setup involves focusing a laser beam into the sample with a high numerical aperture objective, thus forming a diffraction-limited focal volume. The fluorescence of molecules in this region of the sample is collected through the same objective; out-of-focus light is removed with a pinhole in the image plane of the microscope; and the signal is recorded with sensitive detectors, such as avalanche photodiodes. The resulting intensity autocorrelation function normalized by the mean intensity squared can be approximated by

$$G(\tau) = 1 + \frac{1}{\langle N_{obs}\rangle}\left(1+\frac{\tau}{\tau_D}\right)^{-1}\left(1+\frac{\tau}{s^2\tau_D}\right)^{-1/2}\left(1+Ke^{-\tau/\tau_r}\right), \tag{9}$$

where $\langle N_{\mathrm{obs}}\rangle$ is the average number of molecules in the observed volume, τ_{D} is the average time it takes a molecule to diffuse through the observation volume, $s = w_{xy}/w_z$ is the aspect ratio of the lateral and axial dimensions of the volume, and K is the equilibrium constant of a reaction with a relaxation time τ_{r} resulting in fluctuations of the emission intensity. In this case, there are thus two mechanisms contributing to the observed intensity fluctuations: diffusion of molecules in and out of the confocal volume, and fluctuations in the concentrations of molecules caused by the reaction, which could, for example, be a protein folding reaction (**Eq. (2)**). From **Eq. (9)**, it is obvious that the observation of reaction dynamics is limited to timescales not much longer than the diffusion timescale, because the diffusive terms will decay to zero for $\tau \gg \tau_{\mathrm{D}}$. To extend the accessible time range, recurrence effects can be used (Hoffmann et al., 2011), or correlation analysis can be applied to the signal recorded from immobilized molecules.

Eq. (9) shows that the amplitude of the correlation function on freely diffusing molecules is inversely proportional to $\langle N_{\mathrm{obs}}\rangle$. On the other hand, the photon statistics will improve with increasing $\langle N_{\mathrm{obs}}\rangle$, and the statistical noise will thus be smaller for larger

[5]More precisely, the spatial dependence of the molecular brightness $b(\vec{r})$ as seen by the detectors is assumed to be Gaussian distributed, i.e., $b(\vec{r}) = b_0\, exp(-2(x^2+y^2)/w_{xy}^2)exp(-2z^2/w_z^2)$, where b_0 is the brightness at $\vec{r}=0$. The magnitude of the confocal volume is defined by $V = \int b(\vec{r})d^3r/b_0 = \pi^{3/2}w_{xy}^2w_z$, and the average number of molecules in the observation volume is $\langle N_{\mathrm{obs}}\rangle = cV$, where c is the concentration of fluorescent molecules in the solution.

$\langle N_{obs} \rangle$. However, the relative fluctuations decrease with increasing concentration and will eventually be dominated by other fluctuations from imperfections of the experimental system (Krichevsky and Bonnet, 2002). In practice, FCS experiments are typically performed at nanomolar concentrations of fluorescently labeled molecules, where on average about one molecule resides in the observation region. However, the probability of having two or more molecules in the confocal volume is already substantial at these concentrations, which leads to some signal averaging and does therefore not permit a complete separation of the signal from individual molecules. To achieve such separation, it is necessary to dilute the solution so that $\langle N_{obs} \rangle \ll 1$ (typically in the range of ~10 to 100 pM), which will result in bursts of photons originating from single molecules diffusing through the confocal volume, separated by intervals with background signal. The fluorescence signal from each molecule can then be identified using suitable threshold criteria (Michalet et al., 2003). The combination of this type of single-molecule detection with FRET (Ha et al., 1996) is a versatile approach for studying intramolecular distances, distance distributions, and dynamics in biomolecules, including protein folding (Haran, 2003; Michalet et al., 2006; Nettels et al., 2024; Schuler and Eaton, 2008) (cf. Section **Single-Molecule Spectroscopy of Protein Folding**).

Single-molecule Förster resonance energy transfer (FRET)

A quantitative test of Förster's theory (Förster, 1948; Van Der Meer et al., 1994) and the experiment that put FRET on the map of biochemistry was published by Stryer and Haugland in 1967 (Stryer and Haugland, 1967). They attached dansyl and naphthyl groups to the termini of polyproline peptides and measured the transfer efficiency between them as a function of the length of the peptide. As predicted for the dipole-dipole coupling between the donor and the acceptor dye (Förster, 1948), they found the transfer efficiency, defined as $E = k_T/(k_T + k_D)$ (see **Fig. 3**A,B), to depend on the inverse sixth power of the inter-chromophore distance r, in agreement with Theodor Förster's famous result (**Fig. 3**C), according to which

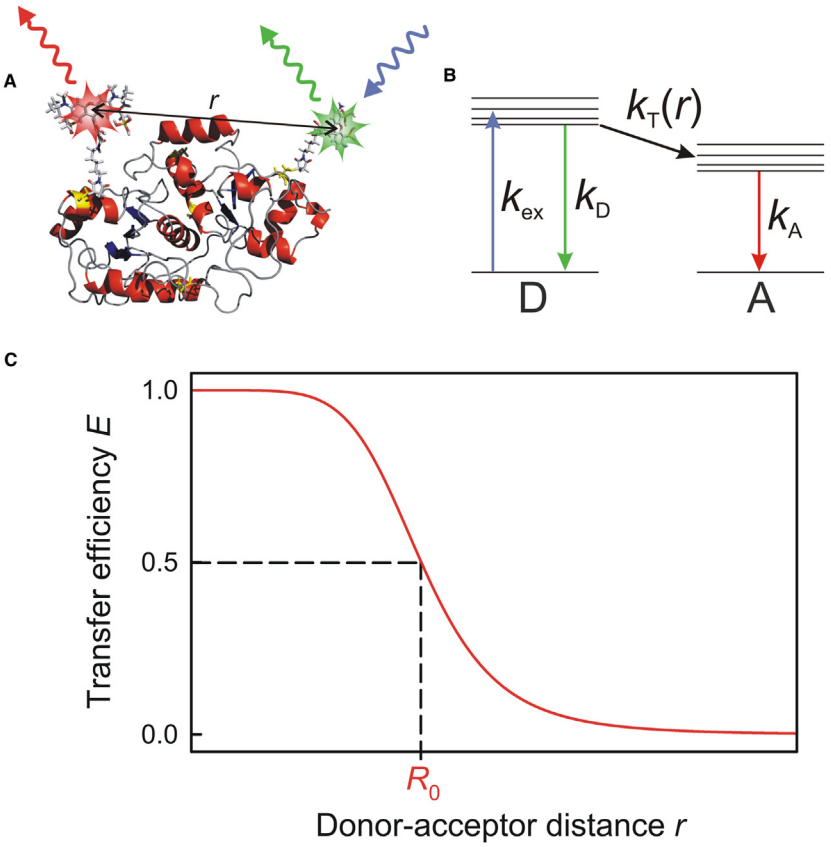

Fig. 3 Förster resonance energy transfer (FRET). (A) Cartoon of a protein molecule labeled with donor and acceptor chromophores. The donor fluorophore (green) can be excited specifically (blue). It can then either emit a fluorescence photon itself or transfer its excitation energy to the acceptor (red). (B) The same process can be depicted in terms of a Jablonsky diagram illustrating the transitions between ground and excited states of donor (D) and acceptor (A). The rate of transfer, k_T, depends on the distance r between donor and acceptor, resulting in the characteristic distance dependence of the transfer efficiency E (C). At the Förster distance R_0, $E = 0.5$. For currently available FRET pairs suitable for single-molecule spectroscopy, R_0 is in the range of 5 nm.

$$E(r) = \frac{R_0^6}{R_0^6 + r^6} \tag{10}$$

where R_0 is the Förster radius, the distance that results in a transfer efficiency of 50 %. R_0 is calculated in Förster's theory as

$$R_0^6 = \frac{9000(\ln 10)\kappa^2 Q_D J}{128\pi^5 n^4 N_A} \tag{11}$$

where $J = \int f_D(\lambda)\epsilon_A(\lambda)\lambda^4 d\lambda$ is the overlap integral between the donor emission spectrum $f_D(\lambda)$ (normalized to an area of one) and the acceptor molar extinction coefficient $\epsilon_A(\lambda)$, Q_D is the donor's fluorescence quantum yield, n is the refractive index of the medium, and N_A is Avogadro's constant (Förster, 1948; Van Der Meer et al., 1994). The orientational factor κ depends on the relative orientation of the chromophores, with $\kappa^2 = (\cos\theta_T - 3\cos\theta_D \cos\theta_A)^2$, where Θ_T is the angle between the donor and acceptor transition dipoles, Θ_D and Θ_A are the angles between the transition moments and the line connecting the centers of donor and acceptor, respectively. In cases where the rotational reorientation of the chromophores is fast compared to the donor excited state lifetime, κ^2 averages to a value of 2/3, significantly simplifying the application of FRET (Haas et al., 1978a; Nüesch et al., 2025). The idea of this "spectroscopic ruler" (Stryer and Haugland, 1967) has had a large impact on the investigation of biomolecular structure and dynamics on distances in the range from about 1 to 10 nm (Haas et al., 1978b; Lakowicz, 1999; Nettels et al., 2024; Selvin, 2000; Stryer, 1978).

Experimentally, transfer efficiencies can be determined in several ways (Van Der Meer et al., 1994), but for single-molecule FRET, two approaches are particularly useful. One is the measurement of the fluorescence intensities from both the donor and the acceptor chromophores, and the calculation of the transfer efficiency according to

$$E = \frac{n_A}{n_A + n_D}\,, \tag{12}$$

where n_A and n_D are the numbers of photons[6] detected from the acceptor and donor chromophore, respectively, during the observation time, corrected for the quantum yields of the dyes, the efficiencies of the detection system in the corresponding wavelength ranges, and related effects (Deniz et al., 2001; Schuler, 2007). The observation time is usually limited either by the diffusion time through the confocal volume or by bleaching of one of the fluorophores. In a typical free-diffusion experiment, for instance, not more a few hundred photons are detected per molecule, and the transfer efficiency values obtained from **Eq. (12)** are thus stochastically distributed around the true transfer efficiency. The transfer efficiency distributions (histograms) obtained from repeated single-molecule measurements are thus broadened by photon shot noise. It is also important to notice that the transfer efficiencies obtained from **Eq. (12)** represent averages over the observation times. The effect of the finite observation time on the transfer efficiency histograms is discussed in Section **Timescales and Distance Distributions**.

A second approach to determine transfer efficiencies, which can be combined with the first (Eggeling et al., 2001; Gopich and Szabo, 2012; Widengren et al., 2006), is the measurement of the fluorescence lifetime of the donor in the presence (τ_{DA}) and absence (τ_D) of the acceptor, yielding the transfer efficiency as

$$E = 1 - \frac{\tau_{DA}}{\tau_D} \tag{13}$$

These parameters can be calculated from the signal of each individual molecule. Again, sampling of many single molecules will result in distributions of observed transfer efficiencies. In addition to shot-noise broadening, the shape of the transfer efficiency histograms critically depends both on the relative timescales of the processes that influence the transfer rate and on the nature of the underlying distance distribution (Gopich and Szabo, 2009b; Sisamakis et al., 2010).

Timescales and distance distributions

The relative magnitude of the timescales of at least four different processes influence the position and width of the FRET efficiency histogram: (a) the rotational correlation time of the chromophores, (b) the fluorescence lifetime of the donor, (c) the distance fluctuations between donor and acceptor (and thus the dynamics of the molecule they are attached to), and (d) the observation timescale.

The rotational correlation time of the chromophores, τ_c, influences the value of the orientation factor κ^2 (**Eq. 11**): if dye reorientation is sufficiently fast such that the relative orientation of the donor and acceptor dipoles average out while the donor is in the excited state, κ^2 can be assumed to equal 2/3. If, in the other extreme, the donor fluorescence decay is much faster than dye reorientation, a static distribution of relative dye orientations can be assumed. Intermediate cases are difficult to treat analytically (Van Der Meer et al., 1994), and simulations become the method of choice (Hillger et al., 2008; Schröder et al., 2005). $\kappa^2 = 2/3$ is often a good approximation, because the rotational correlation times of typical sterically unhindered dyes are in the range of a few hundred picoseconds, while their fluorescence lifetimes are often in the nanosecond range (although they may be reduced by the transfer process). However, even for cases where $\tau_c \approx \tau_{DA}$, orientational averaging can be sufficient for assuming $\kappa^2 \approx 2/3$ (Haas

[6]Strictly speaking, E defined in this way is a randomly distributed quantity. For the true transfer efficiency, the photon *count rates* from donor and acceptor have to be used.

et al., 1978a; Nüesch et al., 2025). Nevertheless, for any quantitative analysis of FRET experiments, it is crucial to quantify the mobility of the dyes attached to the protein with fluorescence polarization anisotropy measurements (Lakowicz, 1999). While steady-state measurements can usually only provide an indication for the presence or absence of sufficient mobility, time-resolved measurements can be used to extract information about both the rotational correlation time and the presence and degree of steric hindrance (Lipari and Szabo, 1980) and are thus preferred.

Another important pair of timescales are the fluorescence lifetime compared to the relaxation time of interdye distance changes, τ_p. Unless τ_p is much shorter than τ_{DA}, the distribution of transfer rates resulting from the distance distribution will give rise to non-exponential fluorescence decays. If the distance dynamics are slow compared to τ_{DA}, the distance distribution can be obtained directly from fluorescence lifetime distributions using procedures originally established for ensemble experiments (Grinvald et al., 1972; Haas et al., 1978b), which can be applied to individual subpopulations identified in single-molecule experiments (Hoffmann et al., 2007; Laurence et al., 2005; Schuler et al., 2016).

Finally, the relative timescales of the interdye distance changes and the observation time will affect the width of the measured transfer efficiency histograms. As shown by Gopich and Szabo, the observation time must be approximately an order of magnitude smaller than the relaxation time of the donor-acceptor distance to obtain physically meaningful distance distributions or corresponding potentials of mean force directly from the transfer efficiency histograms (Gopich and Szabo, 2003a, 2005b). Otherwise, only the mean value of the transfer efficiency of the respective subpopulation can be used to extract information about the distance distribution, and an independent model for the shape of the distance distribution is needed (see below). In practice, this means that distance distributions can be determined from free-diffusion experiments on proteins if the underlying dynamics are on a timescale above about 1 ms, assuming photon count rates of $\sim 10^5$ s^{-1} typically achieved during fluorescence bursts (Gopich and Szabo, 2003a). A noticeable influence of dynamics on the width, however, is already expected for fluctuations in the 10−100 μs timescale (Gopich and Szabo, 2003a; Schuler et al., 2002). Other methods for quantifying distance dynamics from single-molecule photon statistics are described in Section **Data analysis**.

For many structurally heterogeneous systems, such as unfolded and intrinsically disordered proteins, we are dealing with broad distributions of distances (Schuler et al., 2016). Correspondingly, we have to analyze the mean transfer efficiencies $\langle E \rangle$ from single-molecule FRET efficiency histograms in terms of distance distributions (Best et al., 2007; O'Brien et al., 2009; Schuler et al., 2002; Schuler et al., 2016), i.e., a distance distribution function, $P(r)$. If the functional form of $P(r)$ is unknown, the distance distributions of simple polymer models have been employed as approximations (O'Brien et al., 2009; Schuler et al., 2016; Zheng et al., 2018). The observed transfer efficiency histograms will depend both on $P(r)$ and on the timescales of the processes outlined above. The three physically plausible limits for the possible averaging regimes and the resulting mean transfer efficiencies $\langle E \rangle$ are (Schuler et al., 2005):.

1. If the rotational correlation time, τ_c, of the chromophores is short relative to the fluorescence lifetime τ_{DA} of the donor (i.e., $\kappa^2 = 2/3$), and the dynamics of the peptide chain (with relaxation time τ_p) are slow relative to τ_f,

$$\langle E \rangle = \left\langle \frac{k_T(r)}{k_D + k_T(r)} \right\rangle_r = \int_a^{l_c} E(r) P(r) dr \quad \text{with} \quad E(r) = \left(1 + (r/R_0)^6\right)^{-1}, \tag{14}$$

where $P(r)$ is the normalized inter-dye distance distribution, a is the distance of closest approach of the dyes, l_c is the contour length of the peptide, and R_0 is calculated assuming $\kappa^2 = 2/3$.

2. If $\tau_c \ll \tau_{DA}$ and $\tau_p \ll \tau_{DA}$,[7]

$$\langle E \rangle = \frac{\langle k_T(r) \rangle_r}{k_D + \langle k_T(r) \rangle_r} = \frac{\int_a^{l_c} (R_0/r)^6 P(r) dr}{1 + \int_a^{l_c} (R_0/r)^6 P(r) dr} \tag{15}$$

again assuming $\kappa^2 = 2/3$.

3. If $\tau_c \gg \tau_{DA}$ and $\tau_p \gg \tau_{DA}$,

$$\langle E \rangle = \left\langle \frac{k_T(r,\kappa^2)}{k_D + k_T(r,\kappa^2)} \right\rangle_{r,\kappa^2} = \int_0^4 \int_a^{l_c} E(r,\kappa^2) P(r) p(\kappa^2) dr d\kappa^2$$

$$\text{with } E(r,\kappa^2) = \left(1 + \left(r/R_0(\kappa^2)^6\right)\right)^{-1} \tag{16}$$

[7]Note that the transfer rate, k_T, is according to Förster's theory given by $k_T(r) = k_D(\frac{R_0}{r})^6$, where k_D is the fluorescence decay rate of the donor in the absence of the acceptor (see **Fig. 3**).

The isotropic probability density $P(\kappa^2)$ for the case in which all orientations of the donor and acceptor transition dipoles are equally probable (Dale et al., 1979; Van Der Meer et al., 1994) is

$$P(\kappa^2) = \begin{cases} \frac{1}{2\sqrt{3\kappa^2}} \ln\left(2+\sqrt{3}\right) & 0 < \kappa^2 \leq 1 \\ \frac{1}{2\sqrt{3\kappa^2}} \ln\left(\frac{2+\sqrt{3}}{\sqrt{\kappa^2}+\sqrt{\kappa^2-1}}\right) & 1 < \kappa^2 \leq 4 \end{cases} \quad (17)$$

It is important to keep in mind that even for a molecule with a single fixed distance or very rapid conformational averaging, the resulting FRET efficiency histograms are broadened by shot noise. In practice, however, histograms broader than expected from shot noise alone are often observed. The origin of this excess width is sometimes unclear (Merchant et al., 2007; Schuler et al., 2002) and may contain contributions from fluctuating fluorescence quantum efficiencies due to fluorescence quenching, photobleaching, other photochemical processes, or from instrument effects, such as imperfectly overlapping confocal volumes for donor and acceptor channels. The analysis of photon distributions allows the excess width to be quantified (Gopich and Szabo, 2011; Kalinin et al., 2010), but a detailed interpretation in terms of distance distributions usually requires additional information.

Experimental aspects

Performing a single-molecule FRET experiment on protein folding requires several steps. First, protein samples have to be prepared for labeling, either by chemical synthesis or by recombinant expression in combination with site-directed mutagenesis. After identifying a suitable dye pair, the fluorophores need to be attached to the protein as specifically as possible to avoid chemical heterogeneity (Kapanidis and Weiss, 2002; Nikic and Lemke, 2015; Zosel et al., 2022). The equilibrium and kinetic properties of the labeled protein should then ideally be compared to unlabeled protein to ensure that the folding mechanism is not altered. It is also helpful to prepare control molecules, such as stiff polyproline peptides (Best et al., 2007; Schuler et al., 2005) or double-stranded DNA (Hellenkamp et al., 2018; Kapanidis et al., 2004), with the same dye pair to control for changes in solution conditions or other potential sources of error. After customizing the instrument for the sample, data can either be taken on freely diffusing molecules, or on immobilized molecules, if observation times greater than a few milliseconds are desired. Finally, the data need to be processed to correct for background contributions and other effects, to identify fluorescence bursts in diffusion experiments, to calculate transfer efficiencies, fluorescence lifetimes, fluorescence intensity correlation functions, and other parameters derived from the primary observables (Sisamakis et al., 2010).

Instrumentation and data collection

The instrumentation is based on the optics, detectors and electronics developed for optical single-molecule detection (Böhmer and Enderlein, 2003; Moerner, 2002) and fluorescence correlation spectroscopy (Eigen and Rigler, 1994; Hess et al., 2002; Rigler and Elson, 2001b). Instruments for single-molecule FRET (Selvin and Ha, 2008) typically involve either confocal excitation and detection using pulsed or continuous-wave lasers and single photon avalanche photodiodes (APDs), respectively, or wide-field microscopy with two-dimensional detectors such as sensitive CCD or CMOS cameras, often in combination with total internal reflection fluorescence (TIRF) (Axelrod et al., 1984; Juette et al., 2016; Selvin and Ha, 2008) (**Fig. 4**). Wide-field imaging enables the collection of data from many single molecules in parallel, albeit at lower time resolution—typically in the millisecond range—than in a confocal experiment using APDs.

Fig. 5 shows a schematic with the main optical elements for confocal epifluorescence detection. A laser beam is focused with a high numerical-aperture objective to a diffraction-limited focal spot that serves to excite the labeled molecules. In the simplest experiment, the sample molecules are freely diffusing in solution at very low concentration (typically 10−100 pM), ensuring that the probability of two or more molecules residing in the confocal volume at the same time is negligible. When a molecule diffuses through the laser beam, the donor dye is excited, fluorescence from donor and acceptor is collected through the objective and gets focused onto the pinhole, a small aperture (50−200 μm in diameter) serving as a spatial filter that reduces the size of the observation volume. A dichroic mirror finally separates donor and acceptor emission into the corresponding detectors, from where the data are collected with suitable counting electronics. Modern electronics allow the arrival times of every individual detected photon to be stored with picosecond time resolution and synchronized for all detection channels (Felekyan et al., 2005; Wahl et al., 2007, 2008). This mode of data collection provides maximum flexibility and versatility for data processing. The setup can be extended to sorting photons by additional colors, e.g., if more than two chromophores are used (Clamme and Deniz, 2005; Hohng et al., 2004), or by both color and polarization (Sisamakis et al., 2010; Widengren et al., 2006). The advantage of observing freely diffusing molecules is that perturbations from surface interactions can largely be excluded, but the observation time is limited by the diffusion times of the molecules through the confocal volume. Typically, every molecule is observed for no more than a few milliseconds. The resulting fluorescence bursts can be identified by applying an intensity threshold (Deniz et al., 2001) or more sophisticated algorithms (Eggeling et al., 2001; Nir et al., 2006; Zhang and Yang, 2005). From the identified bursts, transfer efficiency histograms or other signal distributions can be constructed (**Fig. 5**). Alternatively, the molecules can be immobilized on

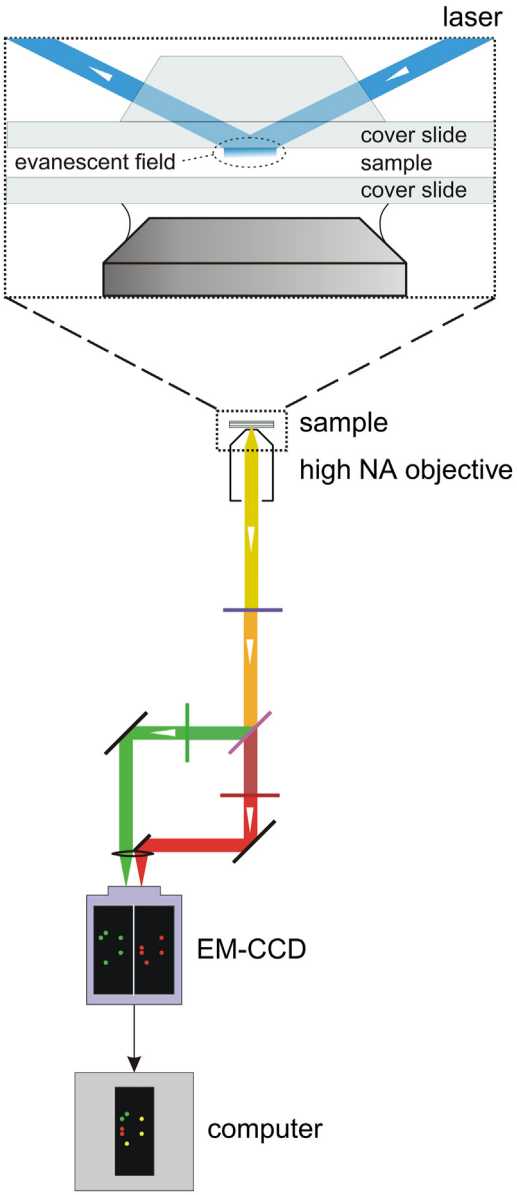

Fig. 4 Schematic of a prism-based total internal reflection fluorescence (TIRF) setup. A laser beam (blue) is reflected at the interface of the sample solution and the top of the sample cell, forming an evanescent field that can be used to selectively excite molecules in close proximity (typically <100 nm) to the surface of the cover slide. The molecules are usually immobilized to the surface. The fluorescence is collected with a high numerical aperture objective lens and focused onto a sensitive CCD camera. An image splitter can be used to direct emission of different wavelengths (e.g., donor and acceptor emission in a FRET experiment) to different areas of the CCD chip, which can then be superimposed for the analysis to quantify donor and acceptor intensities from the same molecule.

the surface and then observed for a more extended period of time, typically for seconds or minutes, until one of the chromophores undergoes photodestruction. In this case, it is important to avoid interactions with the surface that can perturb the sensitive equilibrium of protein folding (Lamichhane et al., 2010; Rasnik et al., 2005). The details of single-molecule instrumentation can be found in several sources (Böhmer and Enderlein, 2003; Michalet et al., 2003; Selvin and Ha, 2008). Confocal and TIRF microscopes for single-molecule detection are commercially available from several manufacturers, and detailed protocols for custom-built instruments are available (Ambrose et al., 2020; Martens et al., 2019; Moya Munoz et al., 2024; Niederauer et al., 2023).

The separation of the signals from various subpopulations, such as the thermodynamic states in protein folding reactions, can be used to measure a variety of parameters (Sisamakis et al., 2010; Widengren et al., 2006) that are difficult to determine otherwise. In confocal experiments with pulsed excitation and four detection channels (Fig. 5), for example, the emission wavelength range (i.e., whether it is a donor or an acceptor photon), the polarization, and the time of emission relative to the excitation pulse become available for every detected photon. Consequently, we can calculate for each burst of photons from a single molecule the transfer

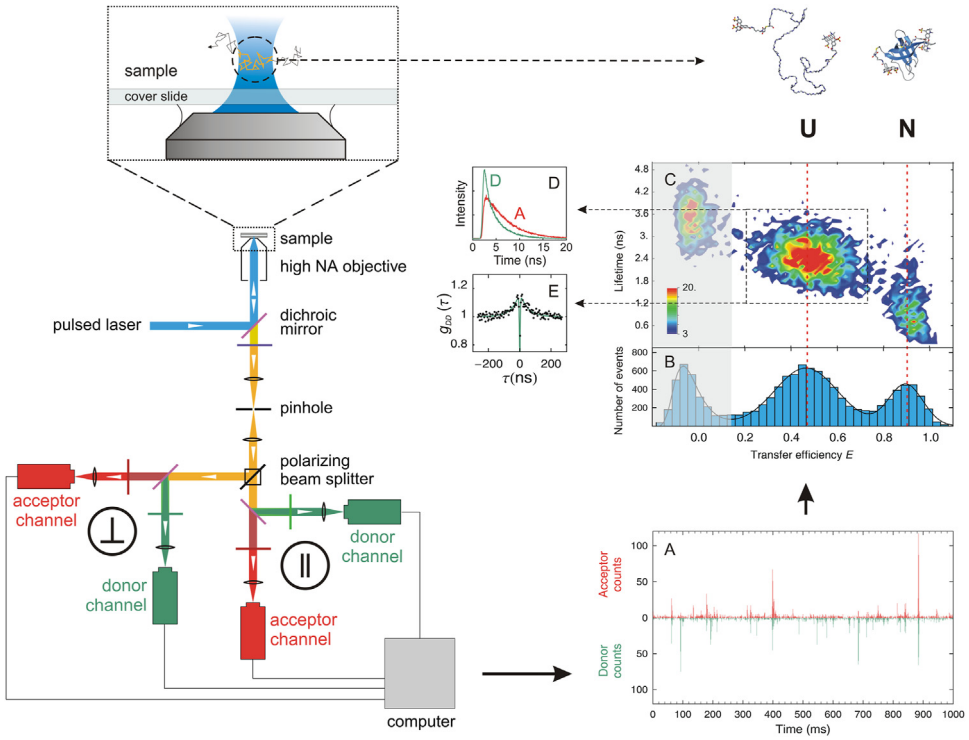

Fig. 5 Schematic of a confocal single-molecule experiment on freely diffusing molecules (left side). In this example, the fluorescence signal is first separated by polarization, and then by wavelength into two detection channels each, corresponding to emission from donor and acceptor chromophores. The right side shows an example of data from an experiment on Csp*Tm* molecules (labeled with Alexa 488 and Alexa 594 fluorophores) freely diffusing in a solution containing 1.5 M guanidinium chloride, conditions close to the unfolding midpoint. One second of a fluorescence intensity measurement (total acquisition time is 60 min) is shown in (A), with bursts of photons originating from individual molecules diffusing through the confocal volume. From each of the bursts (discriminated from background by a combination of thresholds), a transfer efficiency E and a fluorescence lifetime τ (both for donor and acceptor, the donor lifetime is shown in the figure) can be calculated and plotted in a two-dimensional density graph (C). Subpopulations can be selected based on this graph (dashed box) to calculate subpopulation-specific properties, such as fluorescence lifetime decays (D) and correlation functions (E). A one-dimensional histogram of transfer efficiencies is depicted in (B). The plots show populations with mean transfer efficiencies of $E \approx 0.9$ for folded and $E \approx 0.45$ for unfolded molecules. This separation of subpopulations allows changes in transfer efficiencies and other properties to be analyzed individually for each state. The third peak at a transfer efficiency close to zero (shaded) is due to molecules without an active acceptor chromophore. From Schuler, B., Eaton, W.A., 2008. Protein folding studied by single molecule FRET. *Curr. Opin. Struct. Biol.*, 18, 16–26.

efficiency, the donor and acceptor fluorescence lifetimes, the fluorescence anisotropy, and a number of other parameters that aid the interpretation of the results. In a second step, the bursts from subpopulations can be grouped, e.g., to obtain fluorescence decays of an individual subpopulation, devoid of signal contributions from other molecules. The fluorescence lifetime from an individual burst can only be estimated with relatively large uncertainty, but the combination of all photons from a subpopulation can result in decays that are suitable for more detailed analysis.

Protein labeling

To our misfortune, protein chemistry has not made it easy to investigate polypeptides in single-molecule experiments. As of today, even tryptophan, the natural amino acid with the highest fluorescence quantum yield (~0.13), is not suitable for single-molecule detection (unless the molecule contains a very large number of tryptophan residues (Lippitz et al., 2002)) due to its low photostability. The family of fluorescent proteins (Shaner et al., 2005) is usually of limited use for the investigation of protein folding mechanisms because of their relatively large size, their sensitivity to denaturants, and their suboptimal photophysical properties. Labeling with extrinsic fluorophores has thus been unavoidable, but it is complicated by the need for suitable reactive groups for site-specific attachment. For FRET, two (or more) chromophores are needed, and their specific placement on the protein ideally requires groups with orthogonal chemistry. For simple systems, such as short peptides, sequences can be designed to introduce individual copies of residues with suitable reactive side chains (Schuler et al., 2005). In chemical solid phase peptide synthesis, protection groups and the incorporation of non-natural amino acids can be used to increase specificity, but for longer chains, chemical synthesis becomes inefficient and shorter chains have to be ligated (Dawson and Kent, 2000) to obtain the desired product (Deniz

et al., 2000), including semi-synthetic approaches (De Rosa et al., 2013). Considering the versatility of heterologous recombinant protein expression, the production of proteins of virtually any size and sequence in microorganisms is the method of choice to obtain very pure material in sufficiently large amounts for preparative purposes. However, the number of functional groups that can be used for specific labeling is very limited. Sufficiently specific reactivity of natural amino acids is only provided by the sulfhydryl groups of cysteine residues, the amino groups of lysine side chains, and the α-amino group of the N-terminal amino acid. However, except for small peptides, the statistical and therefore often multiple occurrence of cysteine and especially lysine residues in one polypeptide prevents the specific attachment of exactly one label to a protein. For some applications, such as *in vivo* imaging, the degree of labeling is only of secondary importance, but for FRET, specificity is strictly required.

Currently, the most common approach is to rely on cysteine derivatisation owing to its simplicity (Zosel et al., 2022). Increased specificity can be achieved by removing unwanted natural cysteines by site-directed mutagenesis or introducing cysteines with different reactivity due to different molecular environments within the protein (Ratner et al., 2002). Labelling is usually combined with multiple chromatography steps to purify the desired adducts. Alternative methods (Kapanidis and Weiss, 2002) are native chemical ligation of recombinantly expressed and individually labeled protein fragments or intein-mediated protein splicing (David et al., 2004), the specific reaction with thioester derivatives of dyes (Schuler and Pannell, 2002), puromycin-based labeling using in vitro translation (Yamaguchi et al., 2001), or introduction of non-natural amino acids (Cropp and Schultz, 2004; Nikic and Lemke, 2015). A wide variety of suitable organic dyes with various functional groups for protein labeling have become commercially available. Examples of particularly popular chromophores for single-molecule FRET are the cyanine dyes (Mujumdar et al., 1993) or the Alexa Fluor series (Panchuk-Voloshina et al., 1999). Semiconductor quantum dots (Chan et al., 2002) exhibit extreme photostability but are not easily available with single functional groups; so far they can only be used as donors because of their broad absorption spectra; and they are themselves of the size of a small protein, so they have rarely been used for FRET.

Even for the smaller organic dyes, interactions with the protein can interfere with the photophysics of the chromophores or the stability or folding of the protein (Aznauryan et al., 2013). This needs to be taken into account both for the design of the labeled variants and the control experiments. Due to the size of the fluorophores, they are usually positioned on the solvent-exposed surface of the protein. Even then, the use of hydrophobic dyes can reduce the solubility of the protein, or interactions with the protein surface can cause a serious reduction in fluorescence quantum yield, a problem that has been minimized by the introduction of charged groups in many of the popular dyes (Mujumdar et al., 1993; Panchuk-Voloshina et al., 1999). Important control experiments are equilibrium or time-resolved fluorescence anisotropy measurements, which probe the rotational mobility of the dyes and can therefore provide indications for undesirable interactions with the protein surface (Hillger et al., 2008). It is also essential to ensure by direct comparison with unmodified protein that labeling has not substantially altered the protein's stability or folding mechanism.

Data analysis

A large number of different and often complementary types of analysis and theoretical approaches have been applied to single-molecule measurements, which in many cases has been crucial for extracting new information from the experimental data (Barkai et al., 2009). Examples include the use of hidden Markov models (Andrec et al., 2003; Gopich, 2012; Kinz-Thompson et al., 2021; McKinney et al., 2006; Pirchi et al., 2016), information theory (Watkins and Yang, 2005; Yang and Xie, 2002), generating functions (Brown, 2006; Gopich and Szabo, 2003b), concepts of network theory (Baba and Komatsuzaki, 2007; Li et al., 2008, 2009), and more recently machine learning based on deep neural networks (Thomsen et al., 2020; Wanninger et al., 2023) and Bayesian nonparametrics (Pressé and Sgouralis, 2023; Sgouralis et al., 2019).

The analysis of transfer efficiency histograms is often a first step in determining the number of populations and the mean transfer efficiencies from the peak positions. The widths and the shapes of the peaks are often ignored although they may contain useful information about structural heterogeneities and dynamics present within and between the subpopulations (Gopich and Szabo, 2003a). Early theoretical contributions (Deniz et al., 2001; Gopich & Szabo, 2003a, b) culminated in the rigorous treatment of photon statistics in single-molecule experiments by Gopich and Szabo (Gopich and Szabo, 2009b). They showed how to calculate the joint probability $P(n_D, n_A)$ of finding n_D and n_A donor and acceptor photons in a burst and how to obtain from it theoretical transfer efficiency histograms, which can then be compared with the measured ones. Nir et al. (2006) and Antonik et al. (2006) simplified FRET efficiency histogram analysis for rigid molecules by factorizing $P(n_D, n_A)$ into two components, one of them being the distribution of the sum of donor and acceptor photons, which can be taken directly from the measured data and includes the influence of translational diffusion, such that detailed knowledge of the shape of the confocal volume is no longer needed. This type of approach can also be used to analyze single-molecule anisotropy histograms (Kalinin et al., 2007) and heterogeneous mixtures (Kalinin et al., 2008). The method can be used to fit the measured transfer efficiency histograms directly assuming an underlying, shot noise-free, transfer efficiency distribution. Alternatively, this underlying distribution can be obtained from a more general and rigorous maximum likelihood method (Best et al., 2007; Gopich and Szabo, 2007, 2009a).

Conformational dynamics such as the kinetics of protein folding can be obtained from single-molecule FRET data even when the dynamics occur on the same timescale as translational diffusion. With time-binned raw data, kinetic rate constants can be obtained by analyzing transfer efficiency histograms (**Fig. 6**) (Gopich and Szabo, 2007). It is also possible to apply a rigorous maximum likelihood approach to the arrival times and colors of each individual photon (Gopich and Szabo, 2009a). The elegant theoretical framework developed by Gopich and Szabo allows any conformational dynamics or photophysical effects other than FRET to be taken into account (Gopich and Szabo, 2009b). It can also be employed to model rapid conformational dynamics and obtain

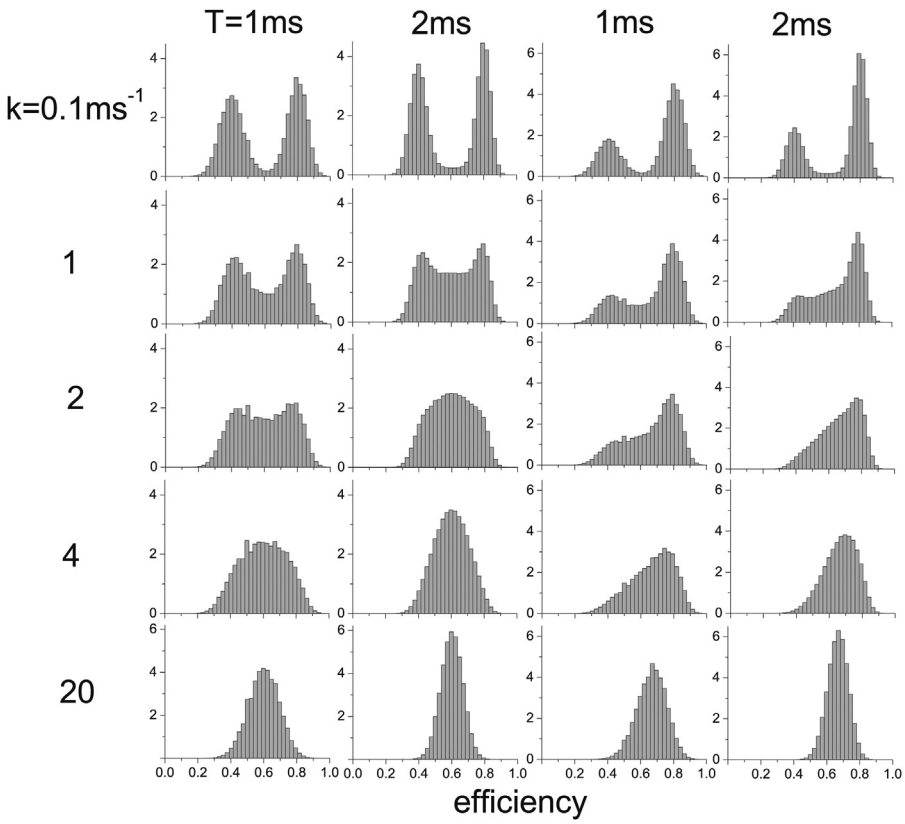

Fig. 6 Effects of conformational dynamics on transfer efficiency histograms in single-molecule FRET experiments on freely diffusing molecules (Gopich and Szabo, 2007). The histograms were calculated assuming that the molecules undergo transitions between two conformational states with low ($E_1 = 0.4$) and high ($E_2 = 0.8$) transfer efficiency. The histograms are shown for different values of the relaxation rate $k = k_1 + k_2$ and the burst duration T. In the first two columns, the equilibrium populations of two the states are equal ($k_1 = k_2$); in the third and fourth columns, the populations differ by a factor of 2 ($k_1 = 2\ k_2$). For low values of k ($kT < 1$), two well-separated peaks are observed, corresponding to the two subpopulations. With increasing relaxation rate, it becomes more likely that a conformational transition occurs during a burst, resulting in an increasing number of events with apparent transfer efficiencies (averaged over T) in the range between the true transfer efficiencies E_1 and E_2. At high relaxation rates ($kT \gg 1$), transitions occur so frequently during a burst that the two subpopulations become indistinguishable. Only one peak remains, whose relative position between E_1 and E_2 is determined by the equilibrium constant $K = k_1/k_2$. Reproduced from Gopich, I.V.; Szabo, A., 2007. Single-molecule FRET with diffusion and conformational dynamics. *J. Phys. Chem. B*, 111, 12925–12932, with permission from ACS Publications.

intramolecular diffusion coefficients from fluorescence intensity correlation functions (Gopich and Szabo, 2005a; Gopich et al., 2009; Nettels et al., 2007) (cf. Section **Unfolded-State Dynamics**).

Single-molecule spectroscopy of protein folding

The exciting prospect of watching individual molecules fold has been a major driving force for single-molecule FRET studies. Additional motivation has come from computer simulations and analytical models of folding, which are playing an increasingly important role in investigations of protein folding mechanisms. If accurate, everything that one could possibly know about a protein folding mechanism is contained in a complete set of folding trajectories from atomistic molecular dynamics calculations, which are now feasible for fast-folding proteins (Lindorff-Larsen et al., 2011; Piana et al., 2014; Voelz et al., 2023). In contrast to ensemble studies, the investigation of individual molecules promises direct access to information on microscopic folding pathways. An ultimate goal of single-molecule FRET studies is the time-resolved observation of individual protein folding events, which will allow the acquisition of trajectories of FRET efficiency—and therefore distance—versus time as the molecule transits between the unfolded and folded states. Such data can provide important insights and can be stringent tests of both simulation and analytical models, thereby speeding progress towards a quantitative and more complete understanding of protein folding mechanisms. **Fig. 1** provides an overview of aspects of protein folding dynamics that have been addressed with single-molecule FRET.

Unfolded state structure and compaction

Förster radii in the range of 5–6 nm for the dye pairs currently available for single-molecule FRET allow the measurement of long-range intramolecular distances and dynamics, and thus make the method ideally suited for investigating unfolded and intrinsically disordered proteins (Schuler et al., 2016), many aspects of which have been difficult to study in detail with ensemble methods because of their large structural heterogeneity. A main advantage that has been exploited in single-molecule experiments is the separation of folded and unfolded subpopulations, thus providing access to the properties of unfolded proteins even at low concentrations of denaturant (Deniz et al., 2000; Schuler et al., 2002), where the majority of molecules in the ensemble are folded. Under these conditions, which are physiologically most relevant, the ensemble-averaged signal would be dominated by the native state. Aspects that have received particular attention are the overall properties of the unfolded state, especially its denaturant-dependent compaction, and the dynamics of the unfolded chain.

The compaction of the unfolded state with decreasing denaturant concentration has been observed for a wide range of proteins (Schuler et al., 2016), including the small cold shock protein Csp*Tm* (Hoffmann et al., 2007; Lipman et al., 2003; Magg and Schmid, 2004; Schuler et al., 2002) (**Fig. 7**), chymotrypsin inhibitor 2 (CI2) (Laurence et al., 2005), for which previous experiments had already been suspected to indicate collapse (Deniz et al., 2000), acyl-CoA binding protein (ACBP) (Laurence et al., 2005), RNase HI (Kuzmenkina et al., 2005, 2006), protein L (Merchant et al., 2007; Sherman and Haran, 2006), the B domain of protein A (Huang et al., 2007), the immunity protein Im9 (Tezuka-Kawakami et al., 2006), and the prion-determining domain of Sup35 (Mukhopadhyay et al., 2007), to name but a few. The growing number of examples showing collapse, and the agreement with the behavior found even for disordered peptides (Buscaglia et al., 2006; Möglich et al., 2006) and small-angle scattering data (Best et al., 2018; Fuertes et al., 2017; Riback et al., 2017) indicates that chain compaction with decreasing denaturant concentration is a generic phenomenon of polypeptides (Best, 2020; Haran, 2012; O'Brien et al., 2008). Kinetic synchrotron radiation circular dichroism experiments provided evidence for the presence of some β-structure in the compact unfolded state (Hoffmann et al., 2007), and kinetic ensemble FRET experiments probing a short segment that forms a β-strand in the folded state indicated the local formation of extended structure in the compact unfolded state of a closely related Csp (Magg et al., 2006). The change of unfolded

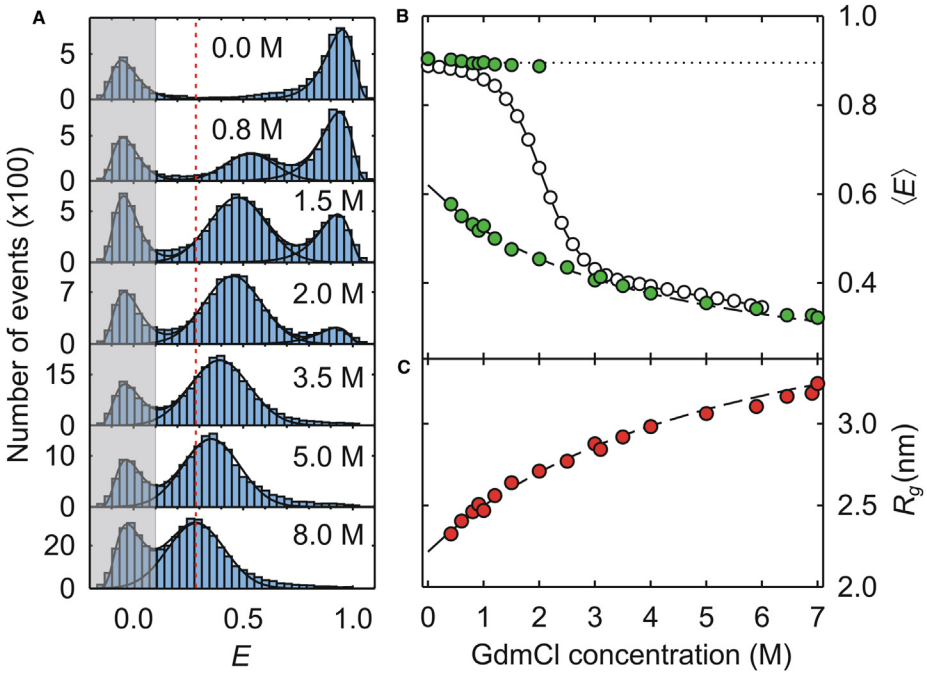

Fig. 7 Unfolded-state compaction from single-molecule FRET. (A) Transfer efficiency histograms of Csp*Tm* labeled with Alexa 488 and 594 at the chain termini at several GdmCl concentrations. The peak at high *E* corresponds to folded protein, the peak at lower *E* to unfolded protein (cf. **Fig. 5**). The signal at $E \approx 0$ originates from molecules with inactive acceptor. (B) Mean transfer efficiencies $\langle E \rangle$ of folded (top, green circles, corrected for refractive index change) and unfolded (bottom, green circles) subpopulations from single-molecule measurements compared to an ensemble unfolding transition of the same sample (white circles) with a two-state fit (black line). (C) Radius of gyration calculated from $\langle E \rangle$ of the unfolded chain assuming the distance distribution of a Gaussian chain, showing the collapse of the unfolded state. Dashed lines are empirical fits to the equivalent of a binding model. Data from Schuler, B., Lipman, E.A., Eaton, W.A., 2002. Probing the free-energy surface for protein folding with single-molecule fluorescence spectroscopy. *Nature*, 419, 743–747. Hoffmann, A., Kane, A., Nettels, D., Hertzog, D.E., Baumgärtel, P., Lengefeld, J., Reichardt, G., Horsley, D.A., Seckler, R., Bakajin, O., Schuler, B., 2007. Mapping protein collapse with single-molecule fluorescence and kinetic synchrotron radiation circular dichroism spectroscopy. *Proc. Natl. Acad. Sci. USA* , 104, 105–110. Nettels, D., Gopich, I.V., Hoffmann, A., Schuler, B., 2007. Ultrafast dynamics of protein collapse from single-molecule photon statistics. *Proc. Natl. Acad. Sci. U. S. A.*, 104, 2655–2660.

state dimensions with denaturant concentration can also be captured by theory and simulations (Borgia et al., 2016; O'Brien et al., 2008; Zheng et al., 2016; Ziv et al., 2009).

In contrast to the rather strong effects of denaturants on unfolded state dimensions, the influence of temperature on the unfolded state is more subtle. A compaction of the unfolded state of a small cold shock protein with increasing temperature was found both in the presence and absence of denaturant (Nettels et al., 2009). While dissociation of denaturant from the polypeptide chain with increasing temperature (Makhatadze and Privalov, 1992) was shown to contribute to compaction, results on a broader range of unfolded and disordered proteins indicated an important role for additional temperature-dependent interactions within the unfolded chain related to the solvation free energy of hydrophilic side chains (Wuttke et al., 2014). Circular dichroism spectroscopy and molecular dynamics simulations indicated changes in secondary structure content with increasing temperature and suggested a contribution of intramolecular hydrogen bonding to unfolded state collapse. Single-molecule experiments have also enabled the observation of the temperature-induced compaction of unfolded frataxin in live cells (Koenig et al., 2015).

Unfolded-state dynamics

Ensemble experiments on short model peptides have provided information about elementary polypeptide dynamics and loop formation on the microsecond timescale and below (Bieri et al., 1999; Lapidus et al., 2000). The importance of these timescales has become particularly obvious through the identification of proteins that fold in a few microseconds (Kubelka et al., 2004). In this regime, the free energy barrier to folding is assumed to be extremely low or even absent, and diffusive chain dynamics become a dominant factor in folding kinetics, posing a speed limit on the folding reaction (Kubelka et al., 2004). An ideal way to probe the dynamics of the heterogeneous ensemble of non-native conformations in proteins is single-molecule spectroscopy: with the Förster radii of currently available dye pairs, single-molecule FRET is sensitive for distance changes in the range of ~3−10 nm, and the absence of ensemble averaging over many molecules allows spontaneous intramolecular distance fluctuations to be observed at equilibrium, without the need for perturbations to synchronize the ensemble.

Chattopadhyay et al. first used FCS to study the dynamics of the denatured state of the intestinal fatty acid binding protein (Chattopadhyay et al., 2005a, b). Two identical chromophores were positioned 48 residues apart in the sequence such that they could undergo self-quenching by contact formation in the denatured state, resulting in fluorescence intensity fluctuations on the timescale of contact formation. The corresponding component in the correlation function was shown to increase as the protein was denatured, and at 3 M GdmCl the relaxation time extracted was 1.6 μs. A similar technique was used to study the dynamics of a 20 amino-acid polypeptide, the Trp-cage (Neuweiler et al., 2005). Here, the quencher was a tryptophan side chain (residue 6), while the extrinsic chromophore was MR121 attached to a nearby lysine (residue 8). The fluorescence correlation curve of the polypeptide exhibited a temperature-dependent relaxation component on the microsecond timescale, which was assigned to the folding/unfolding dynamics. This approach was extended to the study of unstructured glycine-serine peptides and the dependence of their dynamics on solvent viscosity, chain length, and temperature (Neuweiler et al., 2007) and to the analysis of the dynamics of the small binding domain BBL (Neuweiler et al., 2009). Another interesting example for quenching of extrinsic fluorescent dyes by aromatic amino acids was shown for the intrinsically disordered prion-determining domain of Sup35 (Mukhopadhyay et al., 2007), where dynamics on timescales between 20 ns and 300 ns were detected and assigned to quenching of Alexa 488 by the tyrosine residues in the unfolded chain.

An alternative approach to contact quenching is to use the fluctuations in the fluorescence intensity of donor and acceptor undergoing FRET when the distance between them fluctuates in nanosecond fluorescence correlation spectroscopy (nsFCS) (Nettels et al., 2007) (**Fig. 1**F). Subpopulation-specific correlation methods with picosecond time resolution (Nettels et al., 2008; Nettels and Schuler, 2007) can be combined with the information on the dimensions of the unfolded state from subpopulation-specific transfer efficiencies (Schuler et al., 2016) based on a model that describes chain dynamics as a diffusive process on a one-dimensional free energy surface (Gopich and Szabo, 2006; Nettels et al., 2007; Wang and Makarov, 2003). Very rapid reconfiguration times can be extracted, which for CspTm have been found to increase from about 20 ns to 60 ns upon collapse of the chain with decreasing denaturant concentration, reflecting an increase in internal friction (Soranno et al., 2012). The resulting intramolecular diffusion coefficients are a key parameter in Kramers-like descriptions of protein folding (Bryngelson et al., 1995), and the dependence of internal friction on chain dimensions provides an indication for the change in intramolecular dynamics as the protein progresses towards the native state (Best and Hummer, 2006; Chahine et al., 2007). The timescales obtained from this analysis is very similar to the relaxation times calculated from the Rouse and Zimm theories of ideal polymer chains (Grosberg and Khokhlov, 1994). Chain reconfiguration times in the range of 10−100 ns have turned out to be typical for segments of 50−100 residues in unfolded and intrinsically disordered proteins (Schuler et al., 2016).

The existence of a universal diffusion-limited timescale in the dynamics of unfolded proteins has important implications. Firstly, if slower timescales are observed in denatured state dynamics or folding kinetics, this presents an indication for the presence of stable intrachain interactions or the formation of structured intermediates (Bilsel and Matthews, 2006), thus leading to increased internal friction (Hagen et al., 2005; Soranno et al., 2012) or substantial free energy barriers for folding. Secondly, the diffusional timescale of chain dynamics presents a "speed limit" (Hagen et al., 1996; Kubelka et al., 2004) for the folding reaction, because diffusive encounters of different parts of the chain are a prerequisite for the formation of intramolecular interactions. In other words, the reconfiguration time of the chain is closely related to the effective diffusion coefficient of the unfolded protein on its free energy surface for folding. Correspondingly, a speed limit for folding can be estimated from the timescale of chain dynamics based on a simple one-dimensional Kramers-type model of protein folding (Bryngelson et al., 1995). For Csp*Tm*, e.g., this leads to a value

of $(0.4\ \mu s)^{-1}$ (Nettels et al., 2007), which would correspond to the rate of folding in the absence of a significant free energy barrier, i.e., a downhill reaction (Eaton, 1999). This rate is remarkably close to those of the fastest known protein folding reactions, which have been suggested to approach the diffusional speed limit (Cellmer et al., 2007, 2008; Kubelka et al., 2004; Yang and Gruebele, 2003).

Protein folding trajectories, kinetics, and transition paths

A major goal of single-molecule studies is to monitor the transitions between the folded and unfolded states (**Fig. 1**D,E). The first requirement for such experiments is to measure trajectories of proteins undergoing folding and unfolding transitions. Because of the short residence time in the confocal volume for freely diffusing molecules, experiments to monitor trajectories have focused on immobilized proteins. The first experiments by Hochstrasser and coworkers (Jia et al., 1999; Talaga et al., 2000) indicated that the technical challenge in attaching the protein to a glass surface is to avoid artifacts resulting from transient sticking to the surface. Rhoades et al. (Rhoades et al., 2003, 2004) addressed this difficulty by encapsulating the protein in lipid vesicles and attaching the vesicles to the surface and obtained folding/unfolding trajectories of adenylate kinase and Csp*Tm*. The trajectories for adenylate kinase (Rhoades et al., 2003) exhibited broad distributions of step sizes and transition times, indicating a large degree of complexity that was difficult to interpret quantitatively, whereas Csp*Tm* (Rhoades et al., 2004) showed trajectories for individual molecules close to what would be expected for a two-state protein: rapid jumps between high and low FRET states, corresponding to the folded and unfolded molecule states, with a distribution of residence times expected from the ensemble unfolding and folding times, respectively. The jumps between states could not be resolved, and were estimated to occur in $<100\ \mu s$. Kuzmenkina et al. (Kuzmenkina et al., 2005, 2006) immobilized RNase H via biotin and streptavidin to a cross-linked polyethylene glycol ("star PEG") (Groll et al., 2004) coated surface, and showed that the folding/unfolding equilibrium as a function of denaturant concentration is completely reversible and yields thermodynamic parameters for the surface-immobilized protein in good agreement with ensemble experiments for the unlabeled protein. However, similar to the adenylate kinase studies of Rhoades et al. (Rhoades et al., 2003), the fluorescence trajectories were found to be complex, and showed fluctuations over a wide range of FRET efficiencies. From the mean residence times in the folded and unfolded states, rate coefficients (0.01/s) remarkably close to those found in ensemble experiments for the unlabeled protein were obtained. PEG coatings have since become the most common surface passivation strategy, which has enabled fluorescence trajectories to be monitored for minutes with hundreds of transitions, e.g., for the coupled folding and binding of two intrinsically disordered proteins (Zosel et al., 2018, 2020). A particular strength of such measurements is the possibility to detect kinetic heterogeneity, in this case from peptidyl-prolyl cis-trans isomerization in one of the proteins, which leads to different stability of the bound and folded state (Zosel et al., 2018). Based on single-molecule FRET experiments, even complex folding reactions of large proteins have been dissected in great detail, both in terms of equilibrium folding intermediates and folding dynamics (Agam et al., 2024; Dingfelder et al., 2018, 2021). Another advantage of single-molecule spectroscopy is the possibility to identify and characterize even small subpopulations present at only a few percent, as illustrated by the formation of misfolded conformations in the folding of multidomain proteins (Borgia et al., 2011, 2015).

The kinetics of protein folding can also be investigated in nonequilibrium single-molecule measurements, which is particularly important for reactions where folding and unfolding rates are too dissimilar for both to be resolved in surface experiments, or if the dwell times at equilibrium are too long to observe transitions before photobleaching. Sufficiently slow folding reactions can be probed by simple manual mixing and monitoring changes in transfer efficiency histograms from freely diffusing molecules over time, which has for instance been used to investigate the folding kinetics of large proteins on timescales from minutes to hours (Hofmann et al., 2010) and the misfolding of repeat proteins on timescales up to days (Borgia et al., 2011). Faster reactions can be resolved with continuous-flow mixing methods based on microfabricated devices (Lipman et al., 2003; Pfeil et al., 2009; Wunderlich et al., 2013) (**Fig. 8**) or nanopipettes (Orte et al., 2008; White et al., 2006). Timescales down to a few milliseconds can be resolved reliably (Dingfelder et al., 2017; Wunderlich et al., 2013; Yang et al., 2023), in some cases even down to the submillisecond range (Gambin et al., 2011). Higher time resolution is difficult to achieve with this approach since the minimum dwell time of individual molecules flowing through the confocal volume becomes limiting for collecting a sufficient number of photons per molecule.

An important goal of single-molecule experiments has been to resolve transition paths in protein folding, i.e., the actual process of crossing the barrier, which is typically very short compared to the dwell times in the folded and unfolded states but contains most of the interesting mechanistic information (**Fig. 1**D,E). Chung and Eaton pioneered single-molecule FRET experiments for transition path measurements (Chung and Eaton, 2013, 2018; Chung et al., 2009, 2012, 2015) by focusing on the rapid jumps between unfolded and folded states in recordings from surface-immobilized molecules labeled with FRET dyes. By applying a maximum likelihood method (**Fig. 1**G,H), they were able to quantify average transition path times down to the low microsecond range and probe the effect of native versus non-native interactions for the barrier crossing dynamics in direct comparison with molecular dynamics simulations (Chung et al., 2015). Fully resolving these microsecond transition paths has not been possible so far, but transition path time distributions have been quantified for a slower coupled folding and binding reaction (Sturzenegger et al., 2018), and three-color FRET experiments have been shown to enable more complex folding mechanisms to be resolved (Kim and Chung, 2020). Minimizing photophysical effects (Rasnik et al., 2006; Vogelsang et al., 2008) and increasing the photon emission rate, e.g., by plasmonic enhancement (Grabenhorst et al., 2024), will be crucial for increasing time resolution further and for extracting mechanistic information from transition paths.

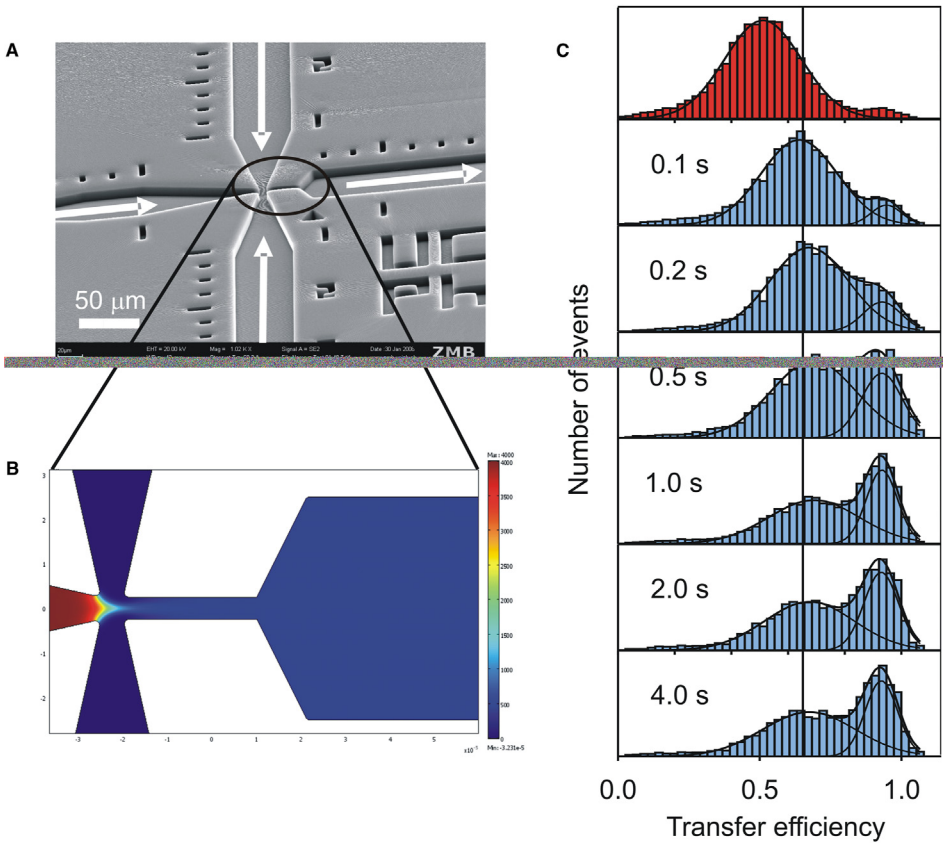

Fig. 8 Protein folding kinetics with single-molecule spectroscopy in a microfluidic mixing device. (A) Electron micrograph of a microfluidic mixing device fabricated by micromolding in silicone (Pfeil et al., 2009). Protein unfolded at high denaturant concentration in the central inlet channel (from the left) is mixed with buffer solutions from the side channels, and the folding reaction can be followed in the observation channel (to the right). (B) A finite element calculation of the mixing process (Wunderlich et al., 2013), indicating the denaturant concentration with a color scale. The narrow mixing region ensures rapid mixing by diffusion. (C) Transfer efficiency histograms of the refolding of Csp*Tm* measured at different positions along the observation channel, corresponding to different times after mixing. The fits to Gaussian distributions having the same peak position and width at all times illustrate the redistribution of populations expected for a two-state system after the initial chain collapse (data taken from (Lipman et al., 2003)). Data for part c from Lipman, E.A., Schuler, B., Bakajin, O., Eaton, W.A., 2003. Single-molecule measurement of protein folding kinetics. *Science*, 301, 1233–1235. Copyright by AAAS.

Closely connected to the measurement of transition paths is the analysis of the different scenarios of "downhill folding". As originally proposed (Bryngelson et al., 1995), downhill folding or unfolding become accessible in kinetic experiments when the bias for the folded or the unfolded state, respectively, becomes sufficiently large (Sabelko et al., 1999; Yang and Gruebele, 2003). By significantly populating all structures along the reaction coordinate, this could simplify the observation of the actual folding process in single protein molecules and the distribution of microscopic pathways taken by a folding protein. In another scenario, only one thermodynamic state exists under a whole range of conditions, resulting in a gradual shifting of a single free energy minimum from unfolded to folded structures (Garcia-Mira et al., 2002; Munoz, 2007). Single-molecule methods are expected to be very helpful in quantifying the structural distributions involved in such "one-state" folding (Munoz, 2007).

Towards protein folding in the cell

Our mechanistic understanding of protein folding in vitro has advanced considerably over the past decades, but the heterogeneous environment of the cell still poses a challenge for quantitative experimental studies in a cellular context. The sensitivity of single-molecule fluorescence in combination with its suitability for investigating heterogeneous conformations presents an opportunity for addressing these questions, and many of the methodological developments in single-molecule spectroscopy of protein folding in vitro can be applied directly to more complex systems.

A simple way of mimicking crowding effects in the cellular environment is by adding crowding agents in vitro, and single-molecule FRET is ideally suited for probing changes in conformations within such concentrated solutions. With this approach, crowding has been shown to compact unfolded proteins (Soranno et al., 2014) and affect the rates of coupled folding and binding between IDPs (Zosel et al., 2020). Another important step towards understanding folding in the cell is the investigation of protein

folding reactions or conformational properties of proteins in the presence of individual purified cellular components, such as molecular chaperones. Early work demonstrated the feasibility of the approach for studying chaperone-substrate and chaperone-chaperone interactions (Taguchi et al., 2001; Yamasaki et al., 1999) and indicated the possibility of obtaining mechanistic information that was not accessible with previous ensemble experiments. Experiments on surface-immobilized GroEL suggested the presence of kinetic intermediates in the reaction cycle of the GroEL/ES system that may be important for increasing the chances for the substrate protein to fold inside the chaperonin chamber before its release (Taguchi et al., 2001; Ueno et al., 2004). Sharma et al. (Sharma et al., 2008) investigated the conformational properties of a variant of maltose binding protein (MBP) upon interaction with the GroEL/ES chaperonin and obtained evidence for the presence of conformational changes in the substrate protein upon binding of ATP to the GroEL-MBP complex and upon interactions with the co-chaperone GroES. Hofmann et al. (Hofmann et al., 2010) found that that confinement in the GroEL/ES cavity decelerates the folding of the C-terminal domain in the substrate protein rhodanese, but leaves the folding rate of the N-terminal domain unaffected, suggesting that a competition between intra- and intermolecular interactions determines the folding rates and mechanisms of a substrate inside the cage.

Single-molecule experiments have also been reported for other chaperone systems. Mickler et al. investigated the conformational dynamics of the Hsp90 chaperone and concluded that the large domain movements of the Hsp90 dimer in the absence of substrate proteins and co-chaperones are dominated by thermal fluctuations and only weakly coupled to ATP hydrolysis (Mickler et al., 2009). Kellner et al. showed that the ATP-dependent binding of multiple DnaK molecules to a non-native substrate protein can lead to a large expansion of the denatured substrate (Kellner et al., 2014). Molecular simulations indicated that hard-core repulsion between the multiple DnaK molecules can disrupt even strong interactions within substrate proteins, which might prepare them for processing by downstream chaperone systems. Banerjee et al. found that the membrane interacting chaperone Hsp27 can modulate the conformations of α-synuclein in the context of a lipid bilayer (Banerjee et al., 2016). The work of Farbman et al. (Farbman et al., 2007) on the interaction of substrate protein with ClpA, which acts as a protein unfoldase in the context of the large protease complex ClpAP in bacteria, shows that single-molecule methods may help to ultimately attain a mechanistic description of protein folding throughout the cellular life cycle of a protein, from its synthesis on the ribosome (Katranidis et al., 2009; Marino et al., 2018) to its degradation. The emerging possibilities to monitor protein folding directly in life cells (Koenig et al., 2015; Sustarsic and Kapanidis, 2015) may enable such processes to be probed directly in the cellular context.

Conclusion

Although single-molecule fluorescence experiments have already contributed substantially to our understanding of protein folding, method development continues to enhance the power of these techniques. Important contributions are expected to come from new protein labeling techniques and fluorophore development, instrumentation, data acquisition, data analysis, simulation, and theory (Nettels et al., 2024). Examples of particularly promising developments from the experimental side are an increased time resolution by plasmonic fluorescence enhancement (Grabenhorst et al., 2024; Nüesch et al., 2022) and advances in data analysis based on deep learning (Thomsen et al., 2020; Wanninger et al., 2023). Another exciting opportunity is the increasing overlap in timescales accessible in single-molecule experiments and molecular simulations (Bottaro and Lindorff-Larsen, 2018; Dimura et al., 2016; Holmstrom et al., 2018), which will enable increasingly detailed mechanistic insight.

References

Agam, G., Barth, A., Lamb, D.C., 2024. Folding pathway of a discontinuous two-domain protein. Nat. Commun. 15 (1), 690.

Ambrose, B., Baxter, J.M., Cully, J., Willmott, M., Steele, E.M., Bateman, B.C., Martin-Fernandez, M.L., Cadby, A., Shewring, J., Aaldering, M., Craggs, T.D., 2020. The smfBox is an open-source platform for single-molecule FRET. Nat. Commun. 11 (1), 5641.

Ambrose, W.P., Goodwin, P.M., Martin, J.C., Keller, R.A., 1994. Single-molecule detection and photochemistry on a surface using near-field optical-excitation. Phys. Rev. Lett. 72 (1), 160—163.

Andrec, M., Levy, R.M., Talaga, D.S., 2003. Direct determination of kinetic rates from single-molecule photon arrival trajectories using hidden Markov models. J. Phys. Chem. A 107 (38), 7454—7464.

Antonik, M., Felekyan, S., Gaiduk, A., Seidel, C.A.M., 2006. Separating structural heterogeneities from stochastic variations in fluorescence resonance energy transfer distributions via photon distribution analysis. J. Phys. Chem. B 110 (13), 6970—6978.

Axelrod, D., Burghardt, T.P., Thompson, N.L., 1984. Total internal-reflection fluorescence. Annu. Rev. Biophys. Bioeng. 13, 247—268.

Aznauryan, M., Nettels, D., Holla, A., Hofmann, H., Schuler, B., 2013. Single-molecule spectroscopy of cold denaturation and the temperature-induced collapse of unfolded proteins. J. Am. Chem. Soc. 135 (38), 14040—14043.

Baba, A., Komatsuzaki, T., 2007. Construction of effective free energy landscape from single-molecule time series. Proc. Natl. Acad. Sci. U. S. A. 104 (49), 19297—19302.

Banerjee, P.R., Deniz, A.A., 2014. Shedding light on protein folding landscapes by single-molecule fluorescence. Chem. Soc. Rev. 43 (4), 1172—1188.

Banerjee, P.R., Moosa, M.M., Deniz, A.A., 2016. Two-dimensional crowding uncovers a hidden conformation of α-synuclein. Angew. Chem. Int. Ed. 55 (41), 12789—12792.

Barkai, E., Brown, F.L.H., Orrit, M., Yang, H., 2009. Theory and Evaluation of Single-Molecule Signals. World Scientific Pub. Co, Singapore.

Berne, B.J., Frisch, H.L., 1967. Light scattering as a probe of fast reaction kinetics. J. Chem. Phys. 47 (9), 3675—&.

Berne, B.J., Pecora, R., 2000. Dynamic Light Scattering. Dover, Mineola, NY.

Best, R., Merchant, K., Gopich, I.V., Schuler, B., Bax, A., Eaton, W.A., 2007. Effect of flexibility and cis residues in single molecule FRET studies of polyproline. Proc. Natl. Acad. Sci. U. S. A. 104 (48), 18964—18969.

Best, R.B., 2020. Emerging consensus on the collapse of unfolded and intrinsically disordered proteins in water. Curr. Opin. Struct. Biol. 60, 27—38.

Best, R.B., Hummer, G., 2006. Diffusive model of protein folding dynamics with Kramers turnover in rate. Phys. Rev. Lett. 96 (22), 228104.

Best, R.B., Zheng, W., Borgia, A., Buholzer, K., Borgia, M.B., Hofmann, H., Soranno, A., Nettels, D., Gast, K., Grishaev, A., Schuler, B., 2018. Comment on "Innovative scattering analysis shows that hydrophobic disordered proteins are expanded in water". Science 361 (6405).
Betzig, E., Chichester, R.J., 1993. Single molecules observed by near-field scanning optical microscopy. Science 262 (5138), 1422—1425.
Bieri, O., Wirz, J., Hellrung, B., Schutkowski, M., Drewello, M., Kiefhaber, T., 1999. The speed limit for protein folding measured by triplet-triplet energy transfer. Proc. Natl. Acad. Sci. U. S. A. 96 (17), 9597—9601.
Bilsel, O., Matthews, C.R., 2006. Molecular dimensions and their distributions in early folding intermediates. Curr. Opin. Struct. Biol. 16 (1), 86—93.
Binnig, G., Quate, C.F., Gerber, C., 1986. Atomic force microscope. Phys. Rev. Lett. 56 (9), 930—933.
Blum, L., Salsburg, Z.W., 1968. Light scattering from a chemically reactive fluid .I. Spectral distribution. J. Chem. Phys. 48 (5), 2292—&.
Böhmer, M., Enderlein, J., 2003. Fluorescence spectroscopy of single molecules under ambient conditions: methodology and technology. ChemPhysChem 4 (8), 793—808.
Borgia, A., Kemplen, K.R., Borgia, M.B., Soranno, A., Shammas, S., Wunderlich, B., Nettels, D., Best, R.B., Clarke, J., Schuler, B., 2015. Transient misfolding dominates multidomain protein folding. Nat. Commun. 6, 8861.
Borgia, A., Zheng, W., Buholzer, K., Borgia, M.B., Schuler, A., Hofmann, H., Soranno, A., Nettels, D., Gast, K., Grishaev, A., Best, R.B., Schuler, B., 2016. Consistent view of polypeptide chain expansion in chemical denaturants from multiple experimental methods. J. Am. Chem. Soc. 138 (36), 11714—11726.
Borgia, M.B., Borgia, A., Best, R.B., Steward, A., Nettels, D., Wunderlich, B., Schuler, B., Clarke, J., 2011. Single-molecule fluorescence reveals sequence-specific misfolding in multidomain proteins. Nature 474 (7353), 662—665.
Bottaro, S., Lindorff-Larsen, K., 2018. Biophysical experiments and biomolecular simulations: a perfect match? Science 361 (6400), 355—360.
Brown, F.L.H., 2006. Generating function methods in single-molecule spectroscopy. Acc. Chem. Res. 39 (6), 363—373.
Bryngelson, J.D., Onuchic, J.N., Socci, N.D., Wolynes, P.G., 1995. Funnels, pathways, and the energy landscape of protein folding: a synthesis. Proteins 21 (3), 167—195.
Buscaglia, M., Lapidus, L.J., Eaton, W.A., Hofrichter, J., 2006. Effects of denaturants on the dynamics of loop formation in polypeptides. Biophys. J. 91 (1), 276—288.
Callen, H.B., Welton, T.A., 1951. Irreversibility and generalized noise. Phys. Rev. 83 (1), 34—40.
Cellmer, T., Henry, E.R., Hofrichter, J., Eaton, W.A., 2008. Measuring internal friction of an ultrafast-folding protein. Proc. Natl. Acad. Sci. U. S. A. 105 (47), 18320—18325.
Cellmer, T., Henry, E.R., Kubelka, J., Hofrichter, J., Eaton, W.A., 2007. Relaxation rate for an ultrafast folding protein is independent of chemical denaturant concentration. J. Am. Chem. Soc. 129 (47), 14564—14565.
Chahine, J., Oliveira, R.J., Leite, V.B.P., Wang, J., 2007. Configuration-dependent diffusion can shift the kinetic transition state and barrier height of protein folding. Proc. Natl. Acad. Sci. U. S. A. 104 (37), 14646—14651.
Chan, W.C., Maxwell, D.J., Gao, X., Bailey, R.E., Han, M., Nie, S., 2002. Luminescent quantum dots for multiplexed biological detection and imaging. Curr. Opin. Biotechnol. 13 (1), 40—46.
Chattopadhyay, K., Elson, E.L., Frieden, C., 2005a. The kinetics of conformational fluctuations in an unfolded protein measured by fluorescence methods. Proc. Natl. Acad. Sci. U. S. A. 102 (7), 2385—2389.
Chattopadhyay, K., Saffarian, S., Elson, E.L., Frieden, C., 2005b. Measuring unfolding of proteins in the presence of denaturant using fluorescence correlation spectroscopy. Biophys. J. 88 (2), 1413—1422.
Chung, H.S., Eaton, W.A., 2013. Single-molecule fluorescence probes dynamics of barrier crossing. Nature 502 (7473), 685—688.
Chung, H.S., Eaton, W.A., 2018. Protein folding transition path times from single molecule FRET. Curr. Opin. Struct. Biol. 48, 30—39.
Chung, H.S., Louis, J.M., Eaton, W.A., 2009. Experimental determination of upper bound for transition path times in protein folding from single-molecule photon-by-photon trajectories. Proc. Natl. Acad. Sci. U. S. A. 106 (29), 11837—11844.
Chung, H.S., McHale, K., Louis, J.M., Eaton, W.A., 2012. Single-molecule fluorescence experiments determine protein folding transition path times. Science 335 (6071), 981—984.
Chung, H.S., Piana-Agostinetti, S., Shaw, D.E., Eaton, W.A., 2015. Structural origin of slow diffusion in protein folding. Science 349 (6255), 1504—1510.
Clamme, J.P., Deniz, A.A., 2005. Three-color single-molecule fluorescence resonance energy transfer. ChemPhysChem 6 (1), 74—77.
Cropp, T.A., Schultz, P.G., 2004. An expanding genetic code. Trends Genet. 20 (12), 625—630.
Dale, R.E., Eisinger, J., Blumberg, W.E., 1979. Orientational freedom of molecular probes—orientation factor in intra-molecular energy-transfer. Biophys. J. 26 (2), 161—193.
David, R., Richter, M.P., Beck-Sickinger, A.G., 2004. Expressed protein ligation. Method and applications. Eur. J. Biochem. 271 (4), 663—677.
Dawson, P.E., Kent, S.B., 2000. Synthesis of native proteins by chemical ligation. Annu. Rev. Biochem. 69, 923—960.
De Rosa, L., Russomanno, A., Romanelli, A., D'Andrea, L.D., 2013. Semi-synthesis of labeled proteins for spectroscopic applications. Molecules 18 (1), 440—465.
Deniz, A.A., Laurence, T.A., Beligere, G.S., Dahan, M., Martin, A.B., Chemla, D.S., Dawson, P.E., Schultz, P.G., Weiss, S., 2000. Single-molecule protein folding: diffusion fluorescence resonance energy transfer studies of the denaturation of chymotrypsin inhibitor 2. Proc. Natl. Acad. Sci. U. S. A. 97 (10), 5179—5184.
Deniz, A.A., Laurence, T.A., Dahan, M., Chemla, D.S., Schultz, P.G., Weiss, S., 2001. Ratiometric single-molecule studies of freely diffusing biomolecules. Annu. Rev. Phys. Chem. 52, 233—253.
Dimura, M., Peulen, T.O., Hanke, C.A., Prakash, A., Gohlke, H., Seidel, C.A., 2016. Quantitative FRET studies and integrative modeling unravel the structure and dynamics of biomolecular systems. Curr. Opin. Struct. Biol. 40, 163—185.
Dingfelder, F., Benke, S., Nettels, D., Schuler, B., 2018. Mapping an equilibrium folding intermediate of the cytolytic pore toxin ClyA with single-molecule FRET. J. Phys. Chem. B 122 (49), 11251—11261.
Dingfelder, F., Macocco, I., Benke, S., Nettels, D., Faccioli, P., Schuler, B., 2021. Slow escape from a helical misfolded state of the pore-forming toxin cytolysin A. JACS Au 1 (8), 1217—1230.
Dingfelder, F., Wunderlich, B., Benke, S., Zosel, F., Zijlstra, N., Nettels, D., Schuler, B., 2017. Rapid microfluidic double-jump mixing device for single-molecule spectroscopy. J. Am. Chem. Soc. 139 (17), 6062—6065.
Drake, B., Prater, C.B., Weisenhorn, A.L., Gould, S.A., Albrecht, T.R., Quate, C.F., Cannell, D.S., Hansma, H.G., Hansma, P.K., 1989. Imaging crystals, polymers, and processes in water with the atomic force microscope. Science 243 (4898), 1586—1589.
Eaton, W.A., 1999. Searching for "downhill scenarios" in protein folding. Proc. Natl. Acad. Sci. U. S. A. 96 (11), 5897—5899.
Eggeling, C., Berger, S., Brand, L., Fries, J.R., Schaffer, J., Volkmer, A., Seidel, C.A., 2001. Data registration and selective single-molecule analysis using multi- parameter fluorescence detection. J. Biotechnol. 86 (3), 163—180.
Eigen, M., Rigler, R., 1994. Sorting single molecules: application to diagnostics and evolutionary biotechnology. Proc. Natl. Acad. Sci. U. S. A. 91 (13), 5740—5747.
Farbman, M.E., Gershenson, A., Licht, S., 2007. Single-molecule analysis of nucleotide-dependent substrate binding by the protein unfoldase ClpA. J. Am. Chem. Soc. 129 (41), 12378—12379.
Felekyan, S., Kuhnemuth, R., Kudryavtsev, V., Sandhagen, C., Becker, W., Seidel, C.A.M., 2005. Full correlation from picoseconds to seconds by time-resolved and time-correlated single photon detection. Rev. Sci. Instrum. 76 (8), 083104.
Förster, T., 1948. Zwischenmolekulare Energiewanderung und Fluoreszenz. Ann. Phys. 6 (2), 55—75.
Fuertes, G., Banterle, N., Ruff, K.M., Chowdhury, A., Mercadante, D., Koehler, C., Kachala, M., Estrada Girona, G., Milles, S., Mishra, A., Onck, P.R., Grater, F., Esteban-Martin, S., Pappu, R.V., Svergun, D.I., Lemke, E.A., 2017. Decoupling of size and shape fluctuations in heteropolymeric sequences reconciles discrepancies in SAXS vs. FRET measurements. Proc. Natl. Acad. Sci. U. S. A. 114 (31), E6342—E6351.
Gambin, Y., Vandelinder, V., Ferreon, A.C., Lemke, E.A., Groisman, A., Deniz, A.A., 2011. Visualizing a one-way protein encounter complex by ultrafast single-molecule mixing. Nat. Methods 8 (3), 239—241.
Garcia-Mira, M.M., Sadqi, M., Fischer, N., Sanchez-Ruiz, J.M., Muñoz, V., 2002. Experimental identification of downhill protein folding. Science 298 (5601), 2191—2195.
Gopich, I., Szabo, A., 2005a. Fluorophore-quencher distance correlation functions from single-molecule photon arrival trajectories. J. Phys. Chem. B 109 (14), 6845—6848.

Gopich, I.V., 2012. Likelihood functions for the analysis of single-molecule binned photon sequences. Chem. Phys. 396, 53—60.
Gopich, I.V., Nettels, D., Schuler, B., Szabo, A., 2009. Protein dynamics from single-molecule fluorescence intensity correlation functions. J. Chem. Phys. 131 (9), 095102.
Gopich, I.V., Szabo, A., 2003a. Single-macromolecule fluorescence resonance energy transfer and free-energy profiles. J. Phys. Chem. B 107 (21), 5058—5063.
Gopich, I.V., Szabo, A., 2003b. Statistics of transitions in single molecule kinetics. J. Chem. Phys. 118 (1), 454—455.
Gopich, I.V., Szabo, A., 2005b. Theory of photon statistics in single-molecule Förster resonance energy transfer. J. Chem. Phys. 122 (014707), 1—18.
Gopich, I.V., Szabo, A., 2006. Theory of the statistics of kinetic transitions with application to single-molecule enzyme catalysis. J. Chem. Phys. 124 (15), 154712.
Gopich, I.V., Szabo, A., 2007. Single-molecule FRET with diffusion and conformational dynamics. J. Phys. Chem. B 111 (44), 12925—12932.
Gopich, I.V., Szabo, A., 2009a. Decoding the pattern of photon colors in single-molecule FRET. J. Phys. Chem. B 113 (31), 10965—10973.
Gopich, I.V., Szabo, A., 2009b. Theory of photon counting in single-molecule spectroscopy. In: Barkai, E., Brown, F.L.H., Orrit, M., Yang, H. (Eds.), Theory and Evaluation of Single-Molecule Signals. World Scientific Pub. Co., Singapore, pp. 1—64.
Gopich, I.V., Szabo, A., 2011. Theory of Single-Molecule FRET Efficiency Histograms, Single-Molecule Biophysics. John Wiley & Sons, Inc., pp. 245—297
Gopich, I.V., Szabo, A., 2012. Theory of the energy transfer efficiency and fluorescence lifetime distribution in single-molecule FRET. Proc. Natl. Acad. Sci. U. S. A. 109 (20), 7747—7752.
Grabenhorst, L., Sturzenegger, F., Hasler, M., Schuler, B., Tinnefeld, P., 2024. Single-molecule FRET at 10 MHz count rates. J. Am. Chem. Soc. 146 (5), 3539—3544.
Grinvald, A., Haas, E., Steinberg, I., 1972. Evaluation of distribution of distances between energy donors and acceptors by fluorescence decay. Proc. Natl. Acad. Sci. U. S. A. 69 (8), 2273—&.
Groll, J., Amirgoulova, E.V., Ameringer, T., Heyes, C.D., Rocker, C., Nienhaus, G.U., Moller, M., 2004. Biofunctionalized, ultrathin coatings of cross-linked star-shaped poly(ethylene oxide) allow reversible folding of immobilized proteins. J. Am. Chem. Soc. 126 (13), 4234—4239.
Grosberg, A.Y., Khokhlov, A.R., 1994. Statistical Physics of Macromolecules. AIP Press, Woodbury, NY.
Ha, T., Enderle, T., Ogletree, D.F., Chemla, D.S., Selvin, P.R., Weiss, S., 1996. Probing the interaction between two single molecules: fluorescence resonance energy transfer between a single donor and a single acceptor. Proc. Natl. Acad. Sci. U. S. A. 93 (13), 6264—6268.
Haas, E., 2005. The study of protein folding and dynamics by determination of intramolecular distance distributions and their fluctuations using ensemble and single-molecule FRET measurements. ChemPhysChem 6 (5), 858—870.
Haas, E., Katchalski-Katzir, E., Steinberg, I.Z., 1978a. Effect of the orientation of donor and acceptor on the probability of energy transfer involving electronic transitions of mixed polarization. Biochemistry 17 (23), 5064—5070.
Haas, E., Katchalskikatzir, E., Steinberg, I.Z., 1978b. Brownian-motion of ends of oligopeptide chains in solution as estimated by energy-transfer between chain ends. Biopolymers 17 (1), 11—31.
Hagen, S.J., Hofrichter, J., Szabo, A., Eaton, W.A., 1996. Diffusion-limited contact formation in unfolded cytochrome c: estimating the maximum rate of protein folding. Proc. Natl. Acad. Sci. U. S. A. 93 (21), 11615—11617.
Hagen, S.J., Qiu, L.L., Pabit, S.A., 2005. Diffusional limits to the speed of protein folding: fact or friction? J. Phys. Condens. Matter 17 (18), S1503—S1514.
Haran, G., 2003. Single-molecule fluorescence spectroscopy of biomolecular folding. J. Phys. Condens. Matter 15 (32), R1291—R1317.
Haran, G., 2012. How, when and why proteins collapse: the relation to folding. Curr. Opin. Struct. Biol. 22 (1), 14—20.
Hellenkamp, B., Schmid, S., Doroshenko, O., Opanasyuk, O., Kuhnemuth, R., Rezaei Adariani, S., Ambrose, B., Aznauryan, M., Barth, A., Birkedal, V., Bowen, M.E., Chen, H., Cordes, T., Eilert, T., Fijen, C., Gebhardt, C., Gotz, M., Gouridis, G., Gratton, E., Ha, T., Hao, P., Hanke, C.A., Hartmann, A., Hendrix, J., Hildebrandt, L.L., Hirschfeld, V., Hohlbein, J., Hua, B., Hubner, C.G., Kallis, E., Kapanidis, A.N., Kim, J.Y., Krainer, G., Lamb, D.C., Lee, N.K., Lemke, E.A., Levesque, B., Levitus, M., McCann, J.J., Naredi-Rainer, N., Nettels, D., Ngo, T., Qiu, R., Robb, N.C., Rocker, C., Sanabria, H., Schlierf, M., Schroder, T., Schuler, B., Seidel, H., Streit, L., Thurn, J., Tinnefeld, P., Tyagi, S., Vandenberk, N., Vera, A.M., Weninger, K.R., Wunsch, B., Yanez-Orozco, I.S., Michaelis, J., Seidel, C.A.M., Craggs, T.D., Hugel, T., 2018. Precision and accuracy of single-molecule FRET measurements-a multi-laboratory benchmark study. Nat. Methods 15 (9), 669—676.
Hess, S.T., Huang, S., Heikal, A.A., Webb, W.W., 2002. Biological and chemical applications of fluorescence correlation spectroscopy: a review. Biochemistry 41 (3), 697—705.
Hillger, F., Hänni, D., Nettels, D., Geister, S., Grandin, M., Textor, M., Schuler, B., 2008. Probing protein-chaperone interactions with single molecule fluorescence spectroscopy. Angew. Chem. Int. Ed. 47, 6184—6188.
Hladky, S.B., Haydon, D.A., 1970. Discreteness of conductance change in bimolecular lipid membranes in the presence of certain antibiotics. Nature 225 (5231), 451—453.
Hoffmann, A., Kane, A., Nettels, D., Hertzog, D.E., Baumgärtel, P., Lengefeld, J., Reichardt, G., Horsley, D.A., Seckler, R., Bakajin, O., Schuler, B., 2007. Mapping protein collapse with single-molecule fluorescence and kinetic synchrotron radiation circular dichroism spectroscopy. Proc. Natl. Acad. Sci. U. S. A. 104 (1), 105—110.
Hoffmann, A., Nettels, D., Clark, J., Borgia, A., Radford, S.E., Clarke, J., Schuler, B., 2011. Quantifying heterogeneity and conformational dynamics from single molecule FRET of diffusing molecules: Recurrence analysis of single particles (RASP). PhysChemChemPhys 13, 1857—1871.
Hofmann, H., Hillger, F., Pfeil, S.H., Hoffmann, A., Streich, D., Haenni, D., Nettels, D., Lipman, E.A., Schuler, B., 2010. Single-molecule spectroscopy of protein folding in a chaperonin cage. Proc. Natl. Acad. Sci. U. S. A. 107 (26), 11793—11798.
Hohng, S., Joo, C., Ha, T., 2004. Single-molecule three-color FRET. Biophys. J. 87 (2), 1328—1337.
Holmstrom, E.D., Holla, A., Zheng, W., Nettels, D., Best, R.B., Schuler, B., 2018. Accurate transfer efficiencies, distance distributions, and ensembles of unfolded and intrinsically disordered proteins from single-molecule FRET. Methods Enzymol. 611, 287—325.
Huang, F., Sato, S., Sharpe, T.D., Ying, L.M., Fersht, A.R., 2007. Distinguishing between cooperative and unimodal downhill protein folding. Proc. Natl. Acad. Sci. U. S. A. 104 (1), 123—127.
Hyeon, C., Lee, J., Yoon, J., Hohng, S., Thirumalai, D., 2012. Hidden complexity in the isomerization dynamics of holliday junctions. Nat. Chem. 4 (11), 907—914.
Jia, Y.W., Talaga, D.S., Lau, W.L., Lu, H.S.M., DeGrado, W.F., Hochstrasser, R.M., 1999. Folding dynamics of single GCN4 peptides by fluorescence resonant energy transfer confocal microscopy. Chem. Phys. 247 (1), 69—83.
Juette, M.F., Terry, D.S., Wasserman, M.R., Altman, R.B., Zhou, Z., Zhao, H., Blanchard, S.C., 2016. Single-molecule imaging of non-equilibrium molecular ensembles on the millisecond timescale. Nat. Methods 13 (4), 341—344.
Kalinin, S., Felekyan, S., Antonik, M., Seidel, C.A., 2007. Probability distribution analysis of single-molecule fluorescence anisotropy and resonance energy transfer. J. Phys. Chem. B 111 (34), 10253—10262.
Kalinin, S., Felekyan, S., Valeri, A., Seidel, C.A., 2008. Characterizing multiple molecular states in single-molecule multiparameter fluorescence detection by probability distribution analysis. J. Phys. Chem. B 112 (28), 8361—8374.
Kalinin, S., Valeri, A., Antonik, M., Felekyan, S., Seidel, C.A., 2010. Detection of structural dynamics by FRET: a photon distribution and fluorescence lifetime analysis of systems with multiple states. J. Phys. Chem. B 114 (23), 7983—7995.
Kapanidis, A.N., Lee, N.K., Laurence, T.A., Doose, S., Margeat, E., Weiss, S., 2004. Fluorescence-aided molecule sorting: analysis of structure and interactions by alternating-laser excitation of single molecules. Proc. Natl. Acad. Sci. U. S. A. 101 (24), 8936—8941.
Kapanidis, A.N., Weiss, S., 2002. Fluorescent probes and bioconjugation chemistries for single-molecule fluorescence analysis of biomolecules. J. Chem. Phys. 117 (24), 10953—10964.
Katranidis, A., Atta, D., Schlesinger, R., Nierhaus, K.H., Choli-Papadopoulou, T., Gregor, I., Gerrits, M., Buldt, G., Fitter, J., 2009. Fast biosynthesis of GFP molecules: a single-molecule fluorescence study. Angew Chem. Int. Ed. Engl. 48 (10), 1758—1761.
Katz, B., Miledi, R., 1970. Membrane noise produced by acetylcholine. Nature 226 (5249), 962—963.
Kellermayer, M.S., Smith, S.B., Granzier, H.L., Bustamante, C., 1997. Folding-unfolding transitions in single titin molecules characterized with laser tweezers. Science 276 (5315), 1112—1116 issn: 0036-8075.

Kellner, R., Hofmann, H., Barducci, A., Wunderlich, B., Nettels, D., Schuler, B., 2014. Single-molecule spectroscopy reveals chaperone-mediated expansion of substrate protein. Proc. Natl. Acad. Sci. USA 111 (37), 13355—13360.
Kim, J.Y., Chung, H.S., 2020. Disordered proteins follow diverse transition paths as they fold and bind to a partner. Science 368 (6496), 1253.
Kinz-Thompson, C.D., Ray, K.K., Gonzalez Jr., R.L., 2021. Bayesian inference: the comprehensive approach to analyzing single-molecule experiments. Annu. Rev. Biophys. 50, 191—208.
Koenig, I., Zarrine-Afsar, A., Aznauryan, M., Soranno, A., Wunderlich, B., Dingfelder, F., Stüber, J.C., Plückthun, A., Nettels, D., Schuler, B., 2015. Single-molecule spectroscopy of protein conformational dynamics in live eukaryotic cells. Nat. Methods 12 (8), 773—779.
Krichevsky, O., Bonnet, G., 2002. Fluorescence correlation spectroscopy: the technique and its applications. Rep. Prog. Phys. 65 (2), 251—297.
Kubelka, J., Hofrichter, J., Eaton, W.A., 2004. The protein folding "speed limit". Curr. Opin. Struct. Biol. 14 (1), 76—88.
Kuzmenkina, E.V., Heyes, C.D., Nienhaus, G.U., 2005. Single-molecule Forster resonance energy transfer study of protein dynamics under denaturing conditions. Proc. Natl. Acad. Sci. USA 102 (43), 15471—15476.
Kuzmenkina, E.V., Heyes, C.D., Nienhaus, G.U., 2006. Single-molecule FRET study of denaturant induced unfolding of RNase H. J. Mol. Biol. 357 (1), 313—324.
Lakowicz, J.R., 1999. Principles of Fluorescence Spectroscopy, second ed. Kluwer Academic/Plenum Publishers, New York.
Lamichhane, R., Solem, A., Black, W., Rueda, D., 2010. Single-molecule FRET of protein-nucleic acid and protein-protein complexes: surface passivation and immobilization. Methods 52 (2), 192—200.
Lapidus, L.J., Eaton, W.A., Hofrichter, J., 2000. Measuring the rate of intramolecular contact formation in polypeptides. Proc. Natl. Acad. Sci. U. S. A. 97 (13), 7220—7225.
Laurence, T.A., Kong, X.X., Jäger, M., Weiss, S., 2005. Probing structural heterogeneities and fluctuations of nucleic acids and denatured proteins. Proc. Natl. Acad. Sci. U. S. A. 102 (48), 17348—17353.
Li, C.B., Yang, H., Komatsuzaki, T., 2008. Multiscale complex network of protein conformational fluctuations in single-molecule time series. Proc. Natl. Acad. Sci. U. S. A. 105 (2), 536—541.
Li, C.B., Yang, H., Komatsuzaki, T., 2009. New quantification of local transition heterogeneity of multiscale complex networks constructed from single-molecule time series. J. Phys. Chem. B 113 (44), 14732—14741.
Lindorff-Larsen, K., Piana, S., Dror, R.O., Shaw, D.E., 2011. How fast-folding proteins fold. Science 334, 517—520.
Lipari, G., Szabo, A., 1980. Effect of librational motion on fluorescence depolarization and nuclear magnetic-resonance relaxation in macromolecules and membranes. Biophys. J. 30 (3), 489—506.
Lipman, E.A., Schuler, B., Bakajin, O., Eaton, W.A., 2003. Single-molecule measurement of protein folding kinetics. Science 301 (5637), 1233—1235.
Lippitz, M., Erker, W., Decker, H., van Holde, K.E., Basche, T., 2002. Two-photon excitation microscopy of tryptophan-containing proteins. Proc. Natl. Acad. Sci. U. S. A. 99 (5), 2772—2777.
Macklin, J.J., Trautman, J.K., Harris, T.D., Brus, L.E., 1996. Imaging and time-resolved spectroscopy of single molecules at an interface. Science 272 (5259), 255—258.
Magde, D., Webb, W.W., Elson, E., 1972. Thermodynamic fluctuations in a reacting system—measurement by fluorescence correlation spectroscopy. Phys. Rev. Lett. 29 (11), 705—&.
Magg, C., Kubelka, J., Holtermann, G., Haas, E., Schmid, F.X., 2006. Specificity of the initial collapse in the folding of the cold shock protein. J. Mol. Biol. 360 (5), 1067—1080.
Magg, C., Schmid, F.X., 2004. Rapid collapse precedes the fast two-state folding of the cold shock protein. J. Mol. Biol. 335 (5), 1309—1323.
Makarov, D.E., 2015. Single Molecule Science—Physical Principles and Models. CRC Press, Boca Raton.
Makhatadze, G.I., Privalov, P.L., 1992. Protein interactions with urea and guanidinium chloride. A calorimetric study. J. Mol. Biol. 226 (2), 491—505 issn: 0022-2836.
Marino, J., Buholzer, K.J., Zosel, F., Nettels, D., Schuler, B., 2018. Charge interactions can dominate coupled folding and binding on the ribosome. Biophys. J. 115, 996—1006.
Martens, K.J.A., van Beljouw, S.P.B., van der Els, S., Vink, J.N.A., Baas, S., Vogelaar, G.A., Brouns, S.J.J., van Baarlen, P., Kleerebezem, M., Hohlbein, J., 2019. Visualisation of dCas9 target search in vivo using an open-microscopy framework. Nat. Commun. 10 (1), 3552.
McKinney, S.A., Joo, C., Ha, T., 2006. Analysis of single-molecule FRET trajectories using hidden Markov modeling. Biophys. J. 91 (5), 1941—1951.
Merchant, K.A., Best, R.B., Louis, J.M., Gopich, I.V., Eaton, W.A., 2007. Characterizing the unfolded states of proteins using single-molecule FRET spectroscopy and molecular simulations. Proc. Natl. Acad. Sci. U. S. A. 104 (5), 1528—1533.
Michalet, X., Kapanidis, A.N., Laurence, T., Pinaud, F., Doose, S., Pflughoefft, M., Weiss, S., 2003. The power and prospects of fluorescence microscopies and spectroscopies. Annu. Rev. Biophys. Biomol. Struct. 32, 161—182.
Michalet, X., Weiss, S., Jäger, M., 2006. Single-molecule fluorescence studies of protein folding and conformational dynamics. Chem. Rev. 106 (5), 1785—1813.
Mickler, M., Hessling, M., Ratzke, C., Buchner, J., Hugel, T., 2009. The large conformational changes of Hsp90 are only weakly coupled to ATP hydrolysis. Nat. Struct. Mol. Biol. 16 (3), 281—286.
Moerner, W.E., 2002. A dozen years of single-molecule spectroscopy in physics, chemistry, and biophysics. J. Phys. Chem. B 106 (5), 910—927.
Moerner, W.E., Kador, L., 1989. Optical-detection and spectroscopy of single molecules in a solid. Phys. Rev. Lett. 62 (21), 2535—2538.
Möglich, A., Joder, K., Kiefhaber, T., 2006. End-to-end distance distributions and intrachain diffusion constants in unfolded polypeptide chains indicate intramolecular hydrogen bond formation. Proc. Natl. Acad. Sci. U. S. A. 103 (33), 12394—12399.
Moya Munoz, G.G., Brix, O., Klocke, P., Harris, P.D., Luna Piedra, J.R., Wendler, N.D., Lerner, E., Zijlstra, N., Cordes, T., 2024. Single-molecule detection and super-resolution imaging with a portable and adaptable 3D-printed microscopy platform (Brick-MIC). Sci. Adv. 10 (39), eado3427.
Mujumdar, R.B., Ernst, L.A., Mujumdar, S.R., Lewis, C.J., Waggoner, A.S., 1993. Cyanine dye labeling reagents: sulfoindocyanine succinimidyl esters. Bioconjug. Chem. 4 (2), 105—111.
Mukhopadhyay, S., Krishnan, R., Lemke, E.A., Lindquist, S., Deniz, A.A., 2007. A natively unfolded yeast prion monomer adopts an ensemble of collapsed and rapidly fluctuating structures. Proc. Natl. Acad. Sci. U. S. A. 104 (8), 2649—2654.
Munoz, V., 2007. Conformational dynamics and ensembles in protein folding. Annu. Rev. Biophys. Biomol. Struct. 36, 395—412.
Nettels, D., Galvanetto, N., Ivanovic, M.T., Nüesch, M., Yang, T.J., Schuler, B., 2024. Single-molecule FRET for probing nanoscale biomolecular dynamics. Nat. Rev. Phys. 6 (10), 587—605.
Nettels, D., Gopich, I.V., Hoffmann, A., Schuler, B., 2007. Ultrafast dynamics of protein collapse from single-molecule photon statistics. Proc. Natl. Acad. Sci. U. S. A. 104 (8), 2655—2660.
Nettels, D., Hoffmann, A., Schuler, B., 2008. Unfolded protein and peptide dynamics investigated with single-molecule FRET and correlation spectroscopy from picoseconds to seconds. J. Phys. Chem. B 112 (19), 6137—6146.
Nettels, D., Müller-Späth, S., Küster, F., Hofmann, H., Haenni, D., Rüegger, S., Reymond, L., Hoffmann, A., Kubelka, J., Heinz, B., Gast, K., Best, R.B., Schuler, B., 2009. Single molecule spectroscopy of the temperature-induced collapse of unfolded proteins. Proc. Natl. Acad. Sci. U. S. A. 106 (49), 20740—20745.
Nettels, D., Schuler, B., 2007. Subpopulation-resolved photon statistics of single-molecule energy transfer dynamics. IEEE J. Sel. Top. Quant. Electron. 13 (4), 990—995.
Neuweiler, H., Doose, S., Sauer, M., 2005. A microscopic view of miniprotein folding: enhanced folding efficiency through formation of an intermediate. Proc. Natl. Acad. Sci. U. S. A. 102 (46), 16650—16655.
Neuweiler, H., Johnson, C.M., Fersht, A.R., 2009. Direct observation of ultrafast folding and denatured state dynamics in single protein molecules. Proc. Natl. Acad. Sci. U. S. A. 106 (44), 18569—18574.
Neuweiler, H., Lollmann, M., Doose, S., Sauer, M., 2007. Dynamics of unfolded polypeptide chains in crowded environment studied by fluorescence correlation spectroscopy. J. Mol. Biol. 365 (3), 856—869.
Nie, S.M., Chiu, D.T., Zare, R.N., 1994. Probing individual molecules with confocal fluorescence microscopy. Science 266 (5187), 1018—1021.

Niederauer, C., Seynen, M., Zomerdijk, J., Kamp, M., Ganzinger, K.A., 2023. The K2: open-source simultaneous triple-color TIRF microscope for live-cell and single-molecule imaging. HardwareX 13, e00404.
Nikic, I., Lemke, E.A., 2015. Genetic code expansion enabled site-specific dual-color protein labeling: superresolution microscopy and beyond. Curr. Opin. Chem. Biol. 28, 164–173.
Nir, E., Michalet, X., Hamadani, K.M., Laurence, T.A., Neuhauser, D., Kovchegov, Y., Weiss, S., 2006. Shot-noise limited single-molecule FRET histograms: comparison between theory and experiments. J. Phys. Chem. B 110 (44), 22103–22124.
Nüesch, M., Ivanovic, M.T., Nettels, D., Best, R.B., Schuler, B., 2025. Accuracy of distance distributions and dynamics from single-molecule FRET. Biophys. J. (in press).
Nüesch, M.F., Ivanovic, M.T., Claude, J.B., Nettels, D., Best, R.B., Wenger, J., Schuler, B., 2022. Single-molecule detection of ultrafast biomolecular dynamics with nanophotonics. J. Am. Chem. Soc. 144 (1), 52–56.
O'Brien, E.P., Morrison, G., Brooks, B.R., Thirumalai, D., 2009. How accurate are polymer models in the analysis of Förster resonance energy transfer experiments on proteins? J. Chem. Phys. 130 (12), 124903.
O'Brien, E.P., Ziv, G., Haran, G., Brooks, B.R., Thirumalai, D., 2008. Effects of denaturants and osmolytes on proteins are accurately predicted by the molecular transfer model. Proc. Natl. Acad. Sci. U. S. A. 105 (36), 13403–13408.
Orrit, M., Bernard, J., 1990. Single pentacene molecules detected by fluorescence excitation in a para-terphenyl crystal. Phys. Rev. Lett. 65 (21), 2716–2719.
Orte, A., Craggs, T.D., White, S.S., Jackson, S.E., Klenerman, D., 2008. Evidence of an intermediate and parallel pathways in protein unfolding from single-molecule fluorescence. J. Am. Chem. Soc. 130 (25), 7898–7907.
Panchuk-Voloshina, N., Haugland, R.P., Bishop-Stewart, J., Bhalgat, M.K., Millard, P.J., Mao, F., Leung, W.Y., 1999. Alexa dyes, a series of new fluorescent dyes that yield exceptionally bright, photostable conjugates. J. Histochem. Cytochem. 47 (9), 1179–1188.
Petrosyan, R., Narayan, A., Woodside, M.T., 2021. Single-molecule force spectroscopy of protein folding. J. Mol. Biol. 433 (20), 167207.
Pfeil, S.H., Wickersham, C.E., Hoffmann, A., Lipman, E.A., 2009. A microfluidic mixing system for single-molecule measurements. Rev. Sci. Instrum. 80 (5), 055105.
Piana, S., Klepeis, J.L., Shaw, D.E., 2014. Assessing the accuracy of physical models used in protein-folding simulations: quantitative evidence from long molecular dynamics simulations. Curr. Opin. Struct. Biol. 24, 98–105.
Pirchi, M., Tsukanov, R., Khamis, R., Tomov, T.E., Berger, Y., Khara, D.C., Volkov, H., Haran, G., Nir, E., 2016. Photon-by-Photon hidden Markov model analysis for microsecond single-molecule FRET kinetics. J. Phys. Chem. B 120 (51), 13065–13075.
Pressé, S., Sgouralis, I., 2023. Data Modeling for the Sciences : Applications, Basics, Computations. Cambridge University Press, Cambridge; New York, NY.
Rasnik, I., McKinney, S.A., Ha, T., 2005. Surfaces and orientations: much to FRET about? Acc. Chem. Res. 38 (7), 542–548.
Rasnik, I., McKinney, S.A., Ha, T., 2006. Nonblinking and long-lasting single-molecule fluorescence imaging. Nat. Methods 3 (11), 891–893.
Ratner, V., Kahana, E., Eichler, M., Haas, E., 2002. A general strategy for site-specific double labeling of globular proteins for kinetic FRET studies. Bioconjug. Chem. 13 (5), 1163–1170.
Rhoades, E., Cohen, M., Schuler, B., Haran, G., 2004. Two-state folding observed in individual protein molecules. J. Am. Chem. Soc. 126 (45), 14686–14687.
Rhoades, E., Gussakovsky, E., Haran, G., 2003. Watching proteins fold one molecule at a time. Proc. Natl. Acad. Sci. U. S. A. 100 (6), 3197–3202.
Riback, J.A., Bowman, M.A., Zmyslowski, A.M., Knoverek, C.R., Jumper, J.M., Hinshaw, J.R., Kaye, E.B., Freed, K.F., Clark, P.L., Sosnick, T.R., 2017. Innovative scattering analysis shows that hydrophobic disordered proteins are expanded in water. Science 358 (6360), 238–241.
Rief, M., Gautel, M., Oesterhelt, F., Fernandez, J.M., Gaub, H.E., 1997. Reversible unfolding of individual titin immunoglobulin domains by AFM. Science 276 (5315), 1109–1112.
Rigler, R., Elson, E.L., 2001a. Fluorescence Correlation Spectroscopy: Theory and Applications. Springer, Berlin.
Rigler, R., Elson, E.S., 2001b. Flourescence Correlation Spectroscopy: Theory and Applications. Springer, Berlin.
Rigler, R., Mets, U., Widengren, J., Kask, P., 1993. Fluorescence correlation spectroscopy with high count rate and low-background—analysis of translational diffusion. Eur. Biophys. J. Biophys. Lett. 22 (3), 169–175.
Sabelko, J., Ervin, J., Gruebele, M., 1999. Observation of strange kinetics in protein folding. Proc. Natl. Acad. Sci. U. S. A. 96 (11), 6031–6036.
Sakmann, B., Neher, E., 1995. Single Channel Recording. Plenum Press.
Schröder, G.F., Alexiev, U., Grubmüller, H., 2005. Simulation of fluorescence anisotropy experiments: probing protein dynamics. Biophys. J. 89 (6), 3757–3770.
Schuler, B., 2007. Application of single molecule Förster resonance energy transfer to protein folding. Methods Mol. Biol. 350, 115–138.
Schuler, B., Eaton, W.A., 2008. Protein folding studied by single-molecule FRET. Curr. Opin. Struct. Biol. 18 (1), 16–26.
Schuler, B., Lipman, E.A., Eaton, W.A., 2002. Probing the free-energy surface for protein folding with single-molecule fluorescence spectroscopy. Nature 419 (6908), 743–747.
Schuler, B., Lipman, E.A., Steinbach, P.J., Kumke, M., Eaton, W.A., 2005. Polyproline and the "spectroscopic ruler" revisited with single molecule fluorescence. Proc. Natl. Acad. Sci. U. S. A. 102, 2754–2759.
Schuler, B., Pannell, L.K., 2002. Specific labeling of polypeptides at amino-terminal cysteine residues using Cy5-benzyl thioester. Bioconjug. Chem. 13 (5), 1039–1043.
Schuler, B., Soranno, A., Hofmann, H., Nettels, D., 2016. Single-molecule FRET spectroscopy and the polymer physics of unfolded and intrinsically disordered proteins. Annu. Rev. Biophys. 45, 207–231.
Selvin, P.R., 2000. The renaissance of fluorescence resonance energy transfer. Nat. Struct. Biol. 7 (9), 730–734.
Selvin, P.R., Ha, T., 2008. Single-Molecule Techniques: A Laboratory Manual. Cold Spring Harbor Laboratory Press, New York.
Sgouralis, I., Madaan, S., Djutanta, F., Kha, R., Hariadi, R.F., Presse, S., 2019. A Bayesian nonparametric approach to single molecule forster resonance energy transfer. J. Phys. Chem. B 123 (3), 675–688.
Shaner, N.C., Steinbach, P.A., Tsien, R.Y., 2005. A guide to choosing fluorescent proteins. Nat. Methods 2 (12), 905–909.
Sharma, S., Chakraborty, K., Muller, B.K., Astola, N., Tang, Y.C., Lamb, D.C., Hayer-Hartl, M., Hartl, F.U., 2008. Monitoring protein conformation along the pathway of chaperonin-assisted folding. Cell 133 (1), 142–153.
Sherman, E., Haran, G., 2006. Coil-globule transition in the denatured state of a small protein. Proc. Natl. Acad. Sci. U. S. A. 103 (31), 11539–11543.
Sisamakis, E., Valeri, A., Kalinin, S., Rothwell, P.J., Seidel, C.A.M., 2010. Accurate single-molecule FRET studies using multiparameter fluorescence detection. Methods Enzymol. 475, 455–514.
Soranno, A., Buchli, B., Nettels, D., Müller-Späth, S., Cheng, R.R., Pfeil, S.H., Hoffmann, A., Lipman, E.A., Makarov, D.E., Schuler, B., 2012. Quantifying internal friction in unfolded and intrinsically disordered proteins with single molecule spectroscopy. Proc. Natl. Acad. Sci. U. S. A. 109 (44), 17800–17806.
Soranno, A., Koenig, I., Borgia, M.B., Hofmann, H., Zosel, F., Nettels, D., Schuler, B., 2014. Single-molecule spectroscopy reveals polymer effects of disordered proteins in crowded environments. Proc. Natl. Acad. Sci. U. S. A. 111 (13), 4874–4879.
Stigler, J., Ziegler, F., Gieseke, A., Gebhardt, J.C., Rief, M., 2011. The complex folding network of single calmodulin molecules. Science 334 (6055), 512–516.
Stryer, L., 1978. Fluorescence energy transfer as a spectroscopic ruler. Annu. Rev. Biochem. 47, 819–846.
Stryer, L., Haugland, R.P., 1967. Energy transfer: a spectroscopic ruler. Proc. Natl. Acad. Sci. U. S. A. 58 (2), 719–726.
Sturzenegger, F., Zosel, F., Holmstrom, E.D., Buholzer, K.J., Makarov, D.E., Nettels, D., Schuler, B., 2018. Transition path times of coupled folding and binding reveal the formation of an encounter complex. Nat. Commun. 9 (1), 4708.
Sustarsic, M., Kapanidis, A.N., 2015. Taking the ruler to the jungle: single-molecule FRET for understanding biomolecular structure and dynamics in live cells. Curr. Opin. Struct. Biol. 34, 52–59.
Taguchi, H., Ueno, T., Tadakuma, H., Yoshida, M., Funatsu, T., 2001. Single-molecule observation of protein-protein interactions in the chaperonin system. Nat. Biotechnol. 19 (9), 861–865.

Talaga, D.S., Lau, W.L., Roder, H., Tang, J., Jia, Y., DeGrado, W.F., Hochstrasser, R.M., 2000. Dynamics and folding of single two-stranded coiled-coil peptides studied by fluorescent energy transfer confocal microscopy. Proc. Natl. Acad. Sci. U. S. A. 97 (24), 13021—13026.
Tezuka-Kawakami, T., Gell, C., Brockwell, D.J., Radford, S.E., Smith, D.A., 2006. Urea-induced unfolding of the immunity protein Im9 monitored by spFRET. Biophys. J. 91 (5), L42—L44.
Thomsen, J., Sletfjerding, M.B., Jensen, S.B., Stella, S., Paul, B., Malle, M.G., Montoya, G., Petersen, T.C., Hatzakis, N.S., 2020. DeepFRET, a software for rapid and automated single-molecule FRET data classification using deep learning. eLife 9.
Tskhovrebova, L., Trinick, J., Sleep, J.A., Simmons, R.M., 1997. Elasticity and unfolding of single molecules of the giant muscle protein titin. Nature 387 (6630), 308—312.
Ueno, T., Taguchi, H., Tadakuma, H., Yoshida, M., Funatsu, T., 2004. GroEL mediates protein folding with a two successive timer mechanism. Mol. Cells 14 (4), 423—434.
Van Der Meer, B.W., Coker III, G., Chen, S.Y.S., 1994. Resonance Energy Transfer: Theory and Data. VCH Publishers, Inc., New York.
Viterbi, A.J., 1967. Error bounds for convolutional codes and an asymptotically optimum decoding algorithm. Ieee T. Inform. Theory. 13 (2), 260—+.
Voelz, V.A., Pande, V.S., Bowman, G.R., 2023. Folding@home: achievements from over 20 years of citizen science herald the exascale era. Biophys. J. 122 (14), 2852—2863.
Vogelsang, J., Kasper, R., Steinhauer, C., Person, B., Heilemann, M., Sauer, M., Tinnefeld, P., 2008. A reducing and oxidizing system minimizes photobleaching and blinking of fluorescent dyes. Angew. Chem., Int. Ed. Engl. 47 (29), 5465—5469.
Wahl, M., Rahn, H.-J., Röhlicke, T., Kell, G., Nettels, D., Hillger, F., Schuler, B., Erdmann, R., 2008. Scalable time-correlated photon counting system with multiple independent input channels. Rev. Sci. Instrum. 79, 123113.
Wahl, M., Rahn, H.J., Gregor, I., Erdmann, R., Enderlein, J., 2007. Dead-time optimized time-correlated photon counting instrument with synchronized, independent timing channels. Rev. Sci. Instrum. 78 (3), 033106.
Wang, Z.S., Makarov, D.E., 2003. Nanosecond dynamics of single polypeptide molecules revealed by photoemission statistics of fluorescence resonance energy transfer: a theoretical study. J. Phys. Chem. B 107 (23), 5617—5622.
Wanninger, S., Asadiatouei, P., Bohlen, J., Salem, C.B., Tinnefeld, P., Ploetz, E., Lamb, D.C., 2023. Deep-LASI: deep-learning assisted, single-molecule imaging analysis of multi-color DNA origami structures. Nat. Commun. 14 (1), 6564.
Watkins, L.P., Yang, H., 2005. Detection of intensity change points in time-resolved single-molecule measurements. J. Phys. Chem. B 109 (1), 617—628.
White, S.S., Balasubramanian, S., Klenerman, D., Ying, L.M., 2006. A simple nanomixer for single-molecule kinetics measurements. Angew. Chem. Int. Ed. 45 (45), 7540—7543.
Widengren, J., Kudryavtsev, V., Antonik, M., Berger, S., Gerken, M., Seidel, C.A.M., 2006. Single-molecule detection and identification of multiple species by multiparameter fluorescence detection. Anal. Chem. 78 (6), 2039—2050.
Wunderlich, B., Nettels, D., Benke, S., Clark, J., Weidner, S., Hofmann, H., Pfeil, S.H., Schuler, B., 2013. Microfluidic mixer designed for performing single-molecule kinetics with confocal detection on timescales from milliseconds to minutes. Nat. Protoc. 8 (8), 1459—1474.
Wuttke, R., Hofmann, H., Nettels, D., Borgia, M.B., Mittal, J., Best, R.B., Schuler, B., 2014. Temperature-dependent solvation modulates the dimensions of disordered proteins. Proc. Natl. Acad. Sci. U. S. A. 111 (14), 5213—5218.
Xie, X.S., Dunn, R.C., 1994. Probing single-molecule dynamics. Science 265 (5170), 361—364.
Yamaguchi, J., Nemoto, N., Sasaki, T., Tokumasu, A., Mimori-Kiyosue, Y., Yagi, T., Funatsu, T., 2001. Rapid functional analysis of protein-protein interactions by fluorescent C-terminal labeling and single-molecule imaging. FEBS Lett. 502 (3), 79—83.
Yamasaki, R., Hoshino, M., Wazawa, T., Ishii, Y., Yanagida, T., Kawata, Y., Higurashi, T., Sakai, K., Nagai, J., Goto, Y., 1999. Single molecular observation of the interaction of GroEL with substrate proteins. J. Mol. Biol. 292 (5), 965—972.
Yang, H., Xie, X.S., 2002. Statistical approaches for probing single-molecule dynamics photon-by-photon. Chem. Phys. 284 (1—2), 423—437.
Yang, T., Buholzer, K.J., Sottini, A., Cao, X., deMello, A., Nettels, D., Schuler, B., 2023. Rapid droplet-based mixing for single-molecule spectroscopy. Nat. Methods 20 (10), 1479—1482.
Yang, W.Y., Gruebele, M., 2003. Folding at the speed limit. Nature 423 (6936), 193—197.
Yeh, Y., Keeler, R.N., 1969. Experimental study of reaction kinetics by light scattering .I. Polarized Rayleigh component. J. Chem. Phys. 51 (3), 1120—&.
Zhang, K., Yang, H., 2005. Photon-by-photon determination of emission bursts from diffusing single chromophores. J. Phys. Chem. B 109 (46), 21930—21937.
Zheng, W., Borgia, A., Buholzer, K., Grishaev, A., Schuler, B., Best, R.B., 2016. Probing the action of chemical denaturant on an intrinsically disordered protein by simulation and experiment. J. Am. Chem. Soc. 138 (36), 11702—11713.
Zheng, W., Zerze, G.H., Borgia, A., Mittal, J., Schuler, B., Best, R.B., 2018. Inferring properties of disordered chains from FRET transfer efficiencies. J. Chem. Phys. 148 (12), 123329.
Ziv, G., Thirumalai, D., Haran, G., 2009. Collapse transition in proteins. Phys. Chem. Chem. Phys. 11 (1), 83—93.
Zoldak, G., Rief, M., 2013. Force as a single molecule probe of multidimensional protein energy landscapes. Curr. Opin. Struct. Biol. 23 (1), 48—57.
Zosel, F., Holla, A., Schuler, B., 2022. Labeling of proteins for single-molecule fluorescence spectroscopy. Methods Mol. Biol. 2376, 207—233.
Zosel, F., Mercadante, D., Nettels, D., Schuler, B., 2018. A proline switch explains kinetic heterogeneity in a coupled folding and binding reaction. Nat. Commun. 9 (1), 3332.
Zosel, F., Soranno, A., Buholzer, K.J., Nettels, D., Schuler, B., 2020. Depletion interactions modulate the binding between disordered proteins in crowded environments. Proc. Natl. Acad. Sci. U.S.A. 117 (24), 13480—13489.